Composites Science and Technology 72 (2012) 121–144

Contents lists available at SciVerse ScienceDirect

Composites Science and Technology

journal homepage: www.elsevier.com/locate/compscitech

Review

Carbon nanotube (CNT)-based composites as electrode material for rechargeable Li-ion batteries: A review

Xian-Ming Liu [a,b], Zhen dong Huang [a], Sei woon Oh [a], Biao Zhang [a], Peng-Cheng Ma [a], Matthew M.F. Yuen [a], Jang-Kyo Kim [a,*]

[a] Department of Mechanical Engineering, Hong Kong University of Science & Technology, Clear Water Bay, Kowloon, Hong Kong
[b] College of Chemistry and Chemical Engineering, Luoyang Normal University, Luoyang 471022, Henan, China

ARTICLE INFO

Article history:
Received 12 June 2011
Received in revised form 28 September 2011
Accepted 15 November 2011
Available online 26 November 2011

Keywords:
A. Carbon nanotubes
A. Nano composites
B. Electrical properties
D. Scanning electron microscopy (SEM)
D. Transmission electron microscopy (TEM)

ABSTRACT

The ever-increasing demands for higher energy density and higher power capacity of Li-ion secondary batteries have led to search for electrode materials whose capacities and performance are better than those available today. Carbon nanotubes (CNTs), because of their unique 1D tubular structure, high electrical and thermal conductivities and extremely large surface area, have been considered as ideal additive materials to improve the electrochemical characteristics of both the anode and cathode of Li-ion batteries with much enhanced energy conversion and storage capacities. Recent development of electrode materials for LIBs has been driven mainly by hybrid nanostructures consisting of Li storage compounds and CNTs. In this paper, recent advances are reviewed of the use of CNTs and the methodologies developed to synthesize CNT-based composites for electrode materials. The physical, transport and electrochemical behaviors of the electrodes made from composites containing CNTs are discussed. The electrochemical performance of LIBs affected by the presence of CNTs in terms of energy and power densities, rate capacity, cyclic life and safety are highlighted in comparison with those without or containing other types of carbonaceous materials. The challenges that remain in using CNTs and CNT-based composites, as well as the prospects for exploiting them in the future are discussed.

Contents

* Corresponding author. Tel.: +852 23587207; fax: +852 23581543.
E-mail address: mejkkim@ust.hk (J.-K. Kim).

0266-3538/$ - see front matter © 2011 Elsevier Ltd. All rights reserved.
doi:10.1016/j.compscitech.2011.11.019

Abbreviations

AB	acetylene black
ACNT	aligned carbon nanotube
C	theoretical capacity
CB	carbon black
CF	carbon fiber
CNT	carbon nanotube
CV	cyclic voltammetry
CVD	chemical vapor deposition
EIS	electrochemical impedance spectra
EVs	electric vehicles
HEVs	hybrid electric vehicles
HRTEM	high resolution transmission electron microscopy
LCO	$LiCoO_2$
ICP	intrinsically conductive polymer
LED	light emitting diode
LFP	$LiFePO_4$
LIB	lithium ion battery
LMO	$LiMn_2O_4$
LNC	$LiNi_{0.7}Co_{0.3}O_2$
NCM	$LiNi_{1/3}Co_{1/3}Mn_{1/3}O_2$
MWCNT	multi-walled carbon nanotube
PANI	polyaniline
PEDOT	poly(3,4-ethylenedioxythiophene)
PVC	poly(N-vinyl carbazole)
PVDF	poly(vinylidene fluoride)
q-CNT	quadrangular carbon nanotube
SEM	scanning electron microscopy
SSB	stationary storage battery
SWCNT	single-walled carbon nanotube
TEM	transmission electron microscopy
UPS	uninterrupted power sources
XRD	X-ray diffraction

1. Introduction

One of the greatest challenges to today's wireless, mobile society is to provide highly-efficient, low cost, and environmentally–friendly energy storage media for powering increasingly diverse applications [1,2]. As the performance of these electronic devices depends largely on the performance of the energy storage media which in turn is affected by the properties of the materials used to synthesize them, significant efforts have been made towards developing new and high-performance materials for battery components. Amongst various energy and power technologies, rechargeable Li-ion batteries (LIB) are a representative of those based on electrochemical energy storage and conversion [3–8]. A typical LIB consists of a negative electrode (i.e. anode, made of graphite), a positive electrode (i.e. cathode, made typically of $LiCoO_2$), and a Li ion conducting electrolyte (see Fig. 1). When the cell is charged, Li ions are extracted from the cathode, move through the electrolyte and are inserted into the anode. Upon discharge, the Li ions are released by the anode and taken up again by the cathode. The electrons pass around the external circuits in opposite directions. The positive electrode half-reaction with charging being forwards is given:

$$LiCoO_2 \leftrightarrows Li_{1-x}CoO_2 + xLi^+ + xe^- \quad (1)$$

while the negative electrode half-reaction is given:

$$xLi^+ + xe^- + 6C \leftrightarrows Li_xC_6 \quad (2)$$

Eqs. (1) and (2) are in units of moles, x is the coefficient typically one for a complete reaction.

Rechargeable LIBs possess many advantages over traditional rechargeable batteries, such as lead acid and Ni–Cd batteries. They include high voltage, high energy-to-weight ratio, i.e. energy density, long cyclic life, no memory effect and slow loss of charge when not in service [1,2]. For these reasons, LIBs are currently the most popular type of battery for powering portable electronic devices and are growing in popularity for defense, automotive and aerospace applications. Although they have shown remarkable commercial successes, the electrodes and their constituent materials are still the subject of intensive research. Diverse range of new applications, such as electric vehicles (EVs), hybrid electric vehicles (HEVs), power tools, uninterrupted power sources (UPS), stationary storage batteries (SSBs), microchips and next-generation wireless communication devices, including 3G mobile phones, are the major driving force behind these research efforts to enhance the ultimate battery performance. In addition to the energy/power density and cyclic performance, safety and cost are two most critical issues that have limited their applications so far in these areas. Because a single type of LIB cannot satisfy all requirements of such a large variety of applications, different types with specific properties and characteristics should be considered. For example, batteries with a high energy capacity are required for high-speed telecommunication devices; whereas batteries with a high power capacity are desirable for EVs, HEVs and power tools.

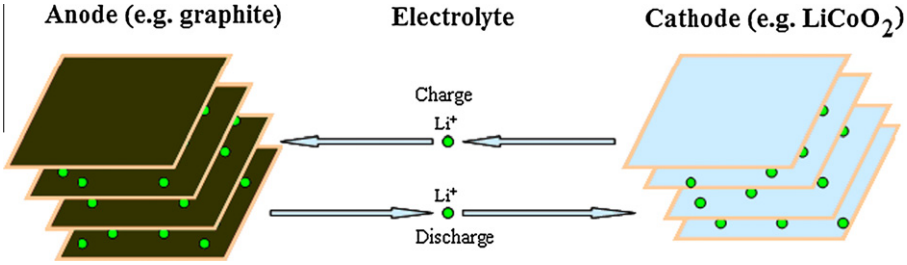

Fig. 1. Working principle of Li-ion batteries. The anode is graphite and cathode is a layered lithiated transition metal oxide. The operation involves a cyclic transfer of Li ions between the electrodes.

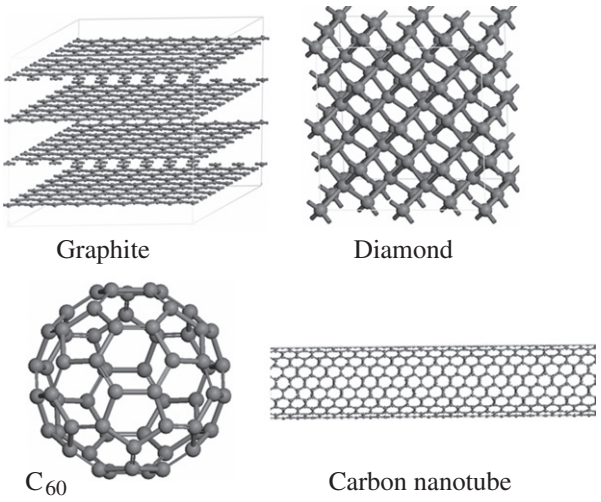

Fig. 2. Structures of different carbon materials. After Lin et al. [17], Moniruzzaman and Winey [18].

A major disadvantage of LIBs is their low power density as a consequence of high polarization, especially at high charge–discharge rates. Slow Li ion diffusion rates, poor electrical and thermal conductions in the electrode and across the electrolyte–electrode interface are mainly responsible for the high polarization. To overcome these problems, it is important to develop new electrode materials with a large surface area, a short diffusion path for ionic transport and high electronic/thermal conductions. Nanoscaled electrode materials offer many advantages over conventional materials: (i) reversible Li intercalation and extraction without destruction of the electrode material structure; (ii) increased Li ion insertion/removal rates due to the short transport path; (iii) enhanced electron transport properties; (iv) increased contact area with the electrolyte, reducing the volume changes associated with intercalation [9,10]. Carbon nanotubes (CNTs) have been used, with varying successes, as additive for both anode and cathode materials, or as the replacement material for anodes, to satisfy the above multi-functional requirements for LIBs [6–8,11–15].

2. Structure, synthesis and properties of CNTs

Since the discovery of CNTs [16], significant research efforts have been directed towards understanding their fundamental properties and practical applications [17,18]. Different from other allotropes of carbon, such as graphite, diamond and fullerene (Fig. 2), CNT is a 1D material with a length-to-diameter ratio, or aspect ratio, in excess of 1000. They are envisioned as cylinders composed of rolled-up graphene sheets around a central hollow core with diameters on a nanometer scale and end caps with a hemisphere of fullerene structure.

There are two types of CNTs: single-walled carbon nanotubes (SWCNTs) and multi-walled carbon nanotubes (MWCNTs) [19]. SWCNTs consist of a single graphene layer, whereas MWCNTs consist of two or more graphene layers with van der Waals forces between adjacent layers. At present, there are primarily four methods developed to synthesize CNTs, including arc-discharge [16,20], laser ablation [21], gas-phase catalytic growth from carbon monoxide [22], and chemical vapor deposition (CVD) from hydrocarbons [23]. The arc discharge and laser ablation techniques make them unsuitable for mass production [24], whereas the gas phase techniques, such as CVD, offer a better potential for production of large quantities of CNTs at a low cost.

According to the rolling angle of the graphene sheet against the tube axis, CNTs have three chiralities: armchair, zigzag and chiral. The chirality is defined by the chiral vector, $C_h = na_1 + ma_2$, where the integers (n, m) are the number of steps along the unit vectors (a_1 and a_2) of the hexagonal lattice [24]. Using this (n, m) naming scheme, the three types of orientation of the carbon atoms around the nanotube circumference are specified. The nanotubes are called "armchair" and "zigzag" for $n = m$ and $m = 0$, respectively; otherwise, they are called "chiral". The chirality of CNTs has a significant impact on their transport properties, particularly the electronic properties. For a given (n, m) CNT, if $(2n + m)$ is a multiple of 3, then it is metallic, otherwise it is a semiconductor. Each MWCNT contains multiple layers of graphene sheets that can have different chiralities, so that the prediction of its electronic properties is more complicated than that of SWCNTs.

The chemical bonding of perfectly structured CNTs is composed entirely of sp^2 carbon–carbon bonds. This bonding structure is stronger than the sp^3 bonds found in diamond, and provides CNTs with amazing mechanical properties. Many studies reported mechanical properties of CNTs that exceed those of any previously known materials [25]. Although there is no consensus on the exact values of these mechanical properties of CNTs, theoretical and experimental results have shown extremely high mechanical properties of CNTs with the Young's modulus as high as 1.2 TPa and the tensile strength of 50–200 GPa [25], making CNTs the strongest and stiffest materials on earth.

In addition to the exceptional mechanical properties, they also possess useful physical properties. Table 1 summarizes these properties that are compared with other carbon materials [26,27]. It is clear that CNTs have many advantages over the other allotropes of carbon in terms of electrical and thermal properties. These properties make CNTs an ideal material for use in areas such as field emission, thermal conductors, energy storage, conductive adhesive, thermal materials, structural materials, fibers, catalyst supports, biological applications, air and water filtration, ceramics and other applications [17,26,28].

Table 1
Physical properties of carbon materials [26,27].

Property	Graphite	Diamond	C_{60}	SWCNT	MWCNT
Gravity (g cm^{-3})	2.09–2.23	3.5	1.7	0.8	1.8
Electrical conductivity (S cm^{-1})	2.5×10^{4}[p] 3.3[c]	10^{-2}	10^{-5}	10^{2}–10^{6}	10^{3}–10^{5}
Thermal conductivity (W/(mK))	3000[p] 6[c]	900–2320	0.4	~6000	~2000
Coefficient of thermal expansion (K^{-1})	-1×10^{-6}[p] 29×10^{-6}[c]	$1\sim3 \times 10^{-6}$	6.2×10^{-5}	Negligible	Negligible
Thermal stability in air (°C)	450–650	777	>600	>600	>600
Surface area (m^2 g^{-1})	Variable	10–50	>100	>100	>100
Modulus (GPa)	1000[p] 36.5[c]	500–1000	14	1200	1000

*p: In-plane and c: *c*-axis.

Recent development of LIBs has involved design of hybrid nanostructures by incorporating CNTs into Li-storage compounds as new electrode material in an effort to best utilize the aforementioned attractive properties of CNTs. Useful properties of CNTs for LIBs include the mechanical and transport properties along with a large specific surface area and a more accessible structure for Li interaction. In contrast, carbon lamellas in carbon black, a traditional additive material, are circumferentially oriented and block much of the particle interior, rendering the majority of matrix useless as intercalation material. In contrast, CNTs with diameters on a nanometer scale and controlled lengths can offer nearly 100% accessibility of the entire carbon structure to Li interaction, especially when the tube ends are opened by simple techniques, such as ball milling [29,30]. The accessibility is often limited if the CNTs are agglomerated, but they still provide inherently a much higher accessibility than any other conventional graphitic materials [13]. The high accessibility of the structure also offer a high mobility to ion exchange processes, a fundamental requirement for dynamic response of batteries based on intercalation.

3. Cathode materials

In rechargeable LIBs, cathode materials are a key component that determines their functional performance. Among many cathode materials, the layer-structured $LiCoO_2$, $LiMnO_2$ and $LiNiO_2$, spinel $LiMn_2O_4$, $Li(Ni_{1/2}Mn_{1/2})O_2$, $Li(Ni_{1/3}Co_{1/3}Mn_{1/3})O_2$, and $Li(Ni_{1/2}Mn_{3/2})O_4$, and elemental sulfur have been studied extensively [31–42]. Li transition metal phosphates with an ordered olivine-type structure, $LiMPO_4$ (M = Fe, Mn, Ni, or Co), have also attracted much attention due to their high theoretical specific capacity (≈170 mA hg^{-1}) [43–45]. Among these phosphates, $LiFePO_4$ is the most attractive because of its high stability, low cost and high compatibility with environment [46,47]. A major disadvantage of $LiFePO_4$ is that to attain the claimed full capacity is extremely difficult because of their low electrical conductivities leading to an initial capacity loss and poor rate capability, as well as slow diffusion rates of Li ions. The electrical and thermal conductivities, and the high stability are amongst the basic characteristics that must be satisfied to ensure high energy storage capability, long lifetime and high safety of LIBs. Li transition metal fluorophosphates, where the $[PO_4]^{3-}$ group is replaced with $[PO_4F]^{4-}$ group have also been considered a promising cathode material because of their enhanced charge balance and dimensionality [48]. Li_2FePO_4F is a new cathode material with several advantages, including facile 2D transport pathways, minimal structural changes during charge–discharge cycles and a high capacity of 135 mA hg^{-1} [49]. These studies redefined the scope of polyanion framework materials as Li insertion cathodes and demonstrated the possibility of using sodium–iron phosphates as starting material for cathodes. A related development is the possibility of a sodium ion cell based on insertion materials such as $Na_3V_2(PO_4)_2F_3$ [50] that possess many advantages, such as improved safety, low cost and possibility of using electrolytes at low decomposition voltages. A new class of Li-based fluorosulphate materials was also developed as cathode materials, which exhibited excellent capacity retention and a high rate at an average potential of 3.6 V versus Li/Li^+. This potential is within the safe stability range of organic electrolytes. The new class of polyanionic compounds with their rich and fascinating crystal chemistry provides valuable information in the quest for even better cathode materials [51].

Although many different types of cathode materials have been developed as discussed above, the most popular chemistries in current production can be narrowed down to three, namely $LiCoO_2$, $LiMn_2O_4$ and $LiFePO_4$. The Li–Co chemistry is more popular in devices like laptops, cameras and cell phones than the other two chemistries mainly because of its higher charge capacity. The other two chemistries are used mainly based on the need for higher discharge currents, improved safety, or where the cost is the driving factor. Judging from the low conductivities of all these three cathode materials, however, carbon-based composites or incorporation of highly conducting carbon materials into these materials have become the choice for future direction in the development of high performance LIBs.

3.1. Layered $LiMO_2$/MWCNT nanocomposites

The layer-structured compound, $LiCoO_2$, has been widely used as very effective cathode material for a long time. However, this material has in general high electrical resistance with reports on serious polarization and poor utilization of active material. In order to make full use of the active material and thus increase the capacity, charge–discharge rate and the lifetime, conductive additives are often added to form conductive networks within the material. Carbon black (CB), carbon fibers (CF) and MWCNTs have been employed as conductive additive and Table 2 compares the electrical resistivities of these three additives and the corresponding electrochemical parameters. MWCNTs are proven to be the most effective in reducing the resistance and thus improving the electrochemical performance of the composite cathode [52]. CNT's 1D geometry and extremely high aspect ratio in particular favor developing continuous conductive networks at a very low percolation threshold, which in turn allow efficient electronic transport throughout the material. Furthermore, the high crystalline and nanoscale structure of MWCNTs facilitate rapid transfer of electrons in comparison with vapor-grown carbon fibers. Their large surface area guarantees close contact with the active material, $LiCoO_2$. Fig. 3 presents schematic models showing the formation and the maintenance of networks in cathode materials containing MWCNTs compared to those containing carbon black. The capacity retention ratios (measured at a rate of 2C) depicted in Fig. 4 clearly indicate the advantage arising from the addition of MWCNTs: the ratio remained almost unchanged for the $LiCoO_2$/MWCNT composite cathode, while the ratios for those containing CF and CB were reduced by 10% and 30%, respectively, after 20 charge–discharge cycles.

A further investigation was carried out of MWCNTs and carbon black as conducting additive in $LiNi_{0.7}Co_{0.3}O_2$ cathodes [53,54]. It is shown that the CNTs acted as conductive networks between $LiNi_{0.7}Co_{0.3}O_2$ particles. The discharge capacity of the composite cathode containing MWCNTs was remarkable 223 mA hg^{-1} with an 89.9% efficiency at C/10 rate and 214 mA hg^{-1} at 1C rate in the initial cycle. This observation further confirmed the effectiveness of CNT addition into the cathode material to improve the electron conduction and reversible capacity along with a high cyclic efficiency. $LiCoO_2$ cathodes with a density of up to 4.0 gcm^{-3} were fabricated using alternate conducting agents of MWCNTs and conventional CB (Super P) [55]. The electrode containing CNTs outperformed that without CNTs in terms of both rate (1C) and cyclic efficiency. A cathode with a high density is one of the most impor-

Table 2
Electrical resistivities of three conductive additives and the corresponding electrochemical parameters. After Wang et al. [52].

Conductive additives	Resistivity of electrode (10^{-2} Ω cm)	Initial discharge capacity (mA hg^{-1})	Capacity retention ratio after 20 cycles (%)
Carbon black (CB)	5500	~85	70
Carbon fibres (CFs)	1000	~104	90
MWCNTs	375	~122	100

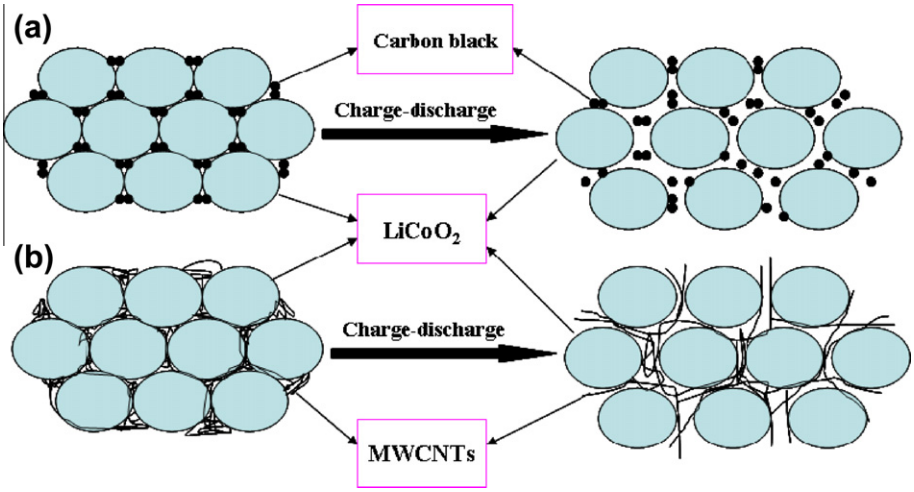

Fig. 3. Schematics of electrodes with different conductive fillers. (a) Carbon black (spherical) and (b) MWCNTs (wire-like). After Wang et al. [52].

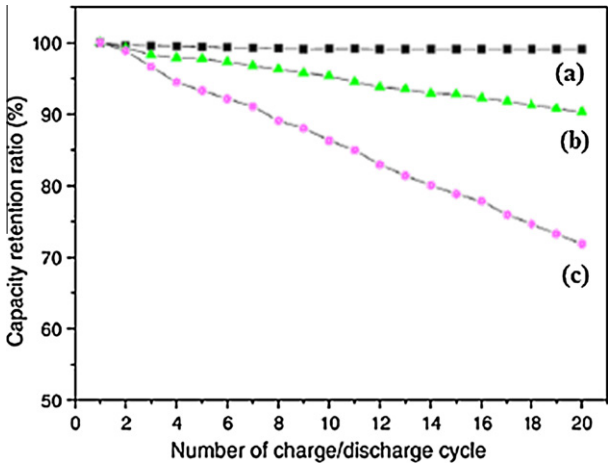

Fig. 4. Effect of conductive additives on the capacity retention ratio at a rate of 2C: (a) MWCNTs; (b) carbon fibers; and (c) carbon black. After Wang et al. [52].

tant factors that affect Li-ion batteries with a high specific energy, while a cathode with a high conductivity is essential to high power. It can be concluded that MWCNTs are an efficient conducting agent to replace CB for high-energy LIBs.

Among many layered metal oxides, $LiNi_{1/3}Co_{1/3}Mn_{1/3}O_2$ (NCM) is considered a very promising cathode material because of its excellent thermal safety characteristics compared to $LiCoO_2$, good capacity in a wide potential range and small volume changes upon cycling [56,57]. NCM has been chosen as the active material for positive electrodes using 1% MWCNTs as conductive agent [58]. MWCNTs were well mixed with the active materials and attached onto the surface of particles, as shown in Fig. 5a. The addition of MWCNTs significantly enhanced the rate performance of NCM-based cathodes at different C-rates between C/5 and 5C. As shown in Fig. 5b, the specific discharge capacities delivered by the cathodes containing MWCNTs were higher than those of the electrodes containing only the ordinary conductive agents at all investigated rates. The effect was more significant at higher current rates – i.e. about 50% higher specific capacity at 5C. After cycling at relatively high currents and returning to C/5, the capacity values remained much the same as the initial values. The incorporation of CNTs of low contents as a conductive additive presented an effective strategy to establish an electrical percolation network in the electrode, resulting in much improved rate capabilities of NCM electrodes.

3.2. $LiFePO_4$/MWCNT nanocomposites

LIBs work when electrons are exchanged simultaneously as a result of intercalation and extraction of Li ions. Both the ion and

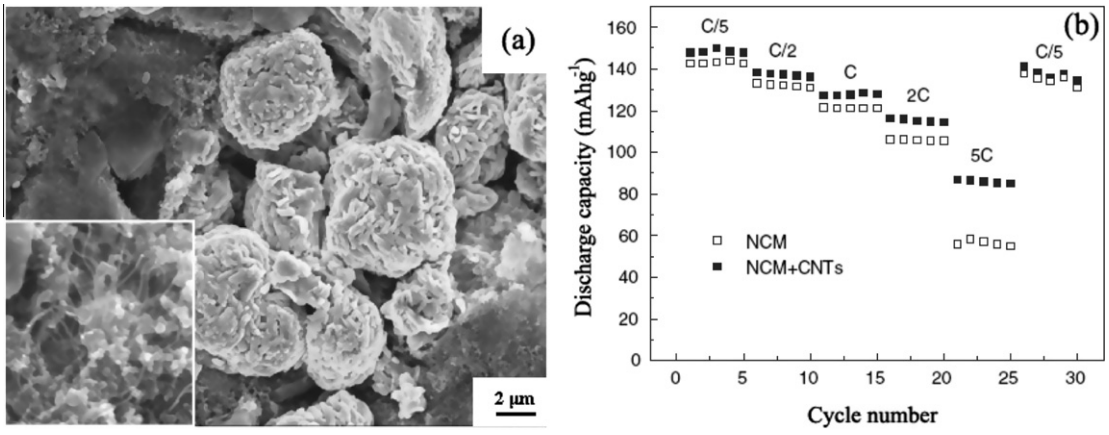

Fig. 5. (a) SEM micrographs of NCM electrodes containing MWCNTs as conductive agent. (b) Rate capability of NCM-based electrodes at different charge/discharge rates. After Varzi et al. [58].

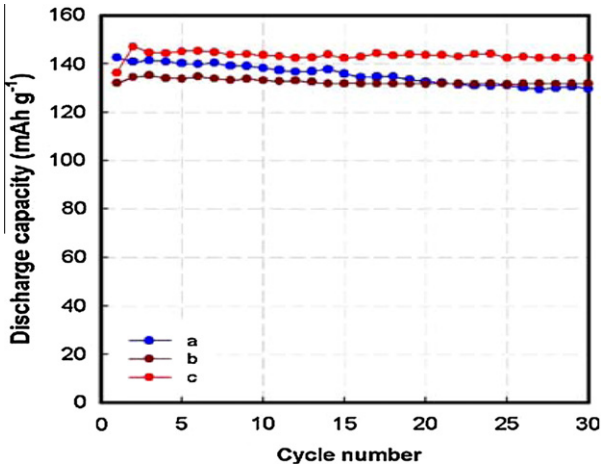

Fig. 6. Cyclic performance of $LiFePO_4$ cathodes containing (a) no additives, (b) 5 wt.% carbon black, and (c) 5 wt.% MWCNT at 0.25 C. After Jin et al. [59].

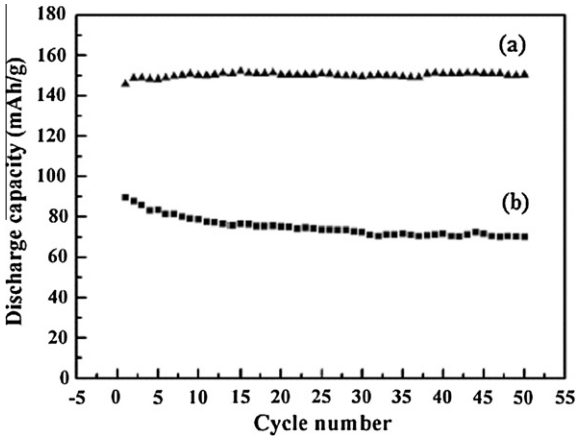

Fig. 8. Cyclic performance of different cathode materials at C/2: (a) $LiFePO_4$ and (b) $LiFePO_4$/1 wt.% MWCNT nanocomposite. After Wang et al. [61].

electron transport properties are critical to cathode materials, and $LiFePO_4$ has a poor electrical conductivity of around 10^{-9} S cm^{-1}. MWCNTs were successfully used to replace the conventional filler, carbon black, in $LiFePO_4$ [59], showing that $LiFePO_4$–C/Li battery with 5 wt.% MWCNTs displayed much better electrochemical properties with a discharge capacity of 142 mA Hg^{-1} at 0.25 C at room temperature than those with carbon black or without any additives (Fig. 6).

A novel network composite cathode made from $LiFePO_4$ particles mixed with MWCNTs was studied for high rate capability [60]. Fig. 7 shows the 3D networks consisting of MWCNTs interconnecting $LiFePO_4$ particles, which effectively improved the electron transfer between the active material and current collector (Al foil), as well as the electrochemical performance, see Table 3. In the high-frequency region, the intercepts with real impedance [Re(Z)] axis of $LiFePO_4$/MWCNTs and $LiFePO_4$/acetylene black composites were 105 Ω and 154 Ω, respectively. These values are known to be the total electric resistance of the electrode materials, electrolyte resistance and electric leads. The substantial reduction in total electrical resistance was attributed to the replacement of acetylene black (AB) by MWCNTs. The slope of the impedance of the $LiFePO_4$/MWCNT composite was higher than that of $LiFePO_4$/AB, indicating enhanced electrochemical activity of $LiFePO_4$ due to MWCNT networks. The initial discharge capacity was improved to 155 mA Hg^{-1} at C/10 rate. MWCNTs were also known very effective in improving rate capability and cyclic efficiency, which is crucial to high-power LIBs particularly for electric vehicles.

In another study on hybrid $LiFePO_4$/MWCNT composites, $LiFePO_4$ was synthesized based on a room-temperature solid-state reaction, followed by microwave heating and addition of both citric acid and MWCNTs [61]. The as-prepared $LiFePO_4$/MWCNT composite cathodes exhibited an excellent electrochemical capacity of 145 mA Hg^{-1} at C/2 and maintained a stable cyclic ability. The cycling behavior of $LiFePO_4$ with and without MWCNT additives are shown in Fig. 8. The initial capacity of $LiFePO_4$ cathodes was reduced from 90 to 70 mA Hg^{-1} after 50 charge–discharge cycles. The large reduction in residual capacity was attributed to the slow diffusion of Li ions in $LiFePO_4$ and poor contact between the $LiFePO_4$ nanoparticles and conductors. In contrast, the corresponding

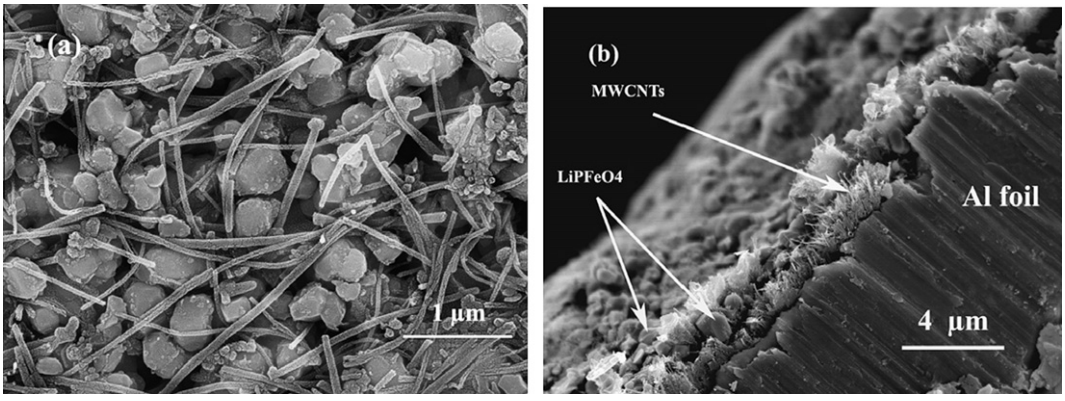

Fig. 7. SEM images of $LiFePO_4$/MWCNTs composite cathode (a: plane section; b: cross section). After Li et al. [60].

Table 3
Two different conductive additives and the corresponding electrochemical parameters. After Li et al. [60].

Conductive additives	Re(Z) of electrode (Ω)	Initial discharge capacity at C/10 (mA Hg^{-1})	Capacity retention ratio after 50 cycles (%)
CB	154	~146	90
MWCNT	105	~155	95

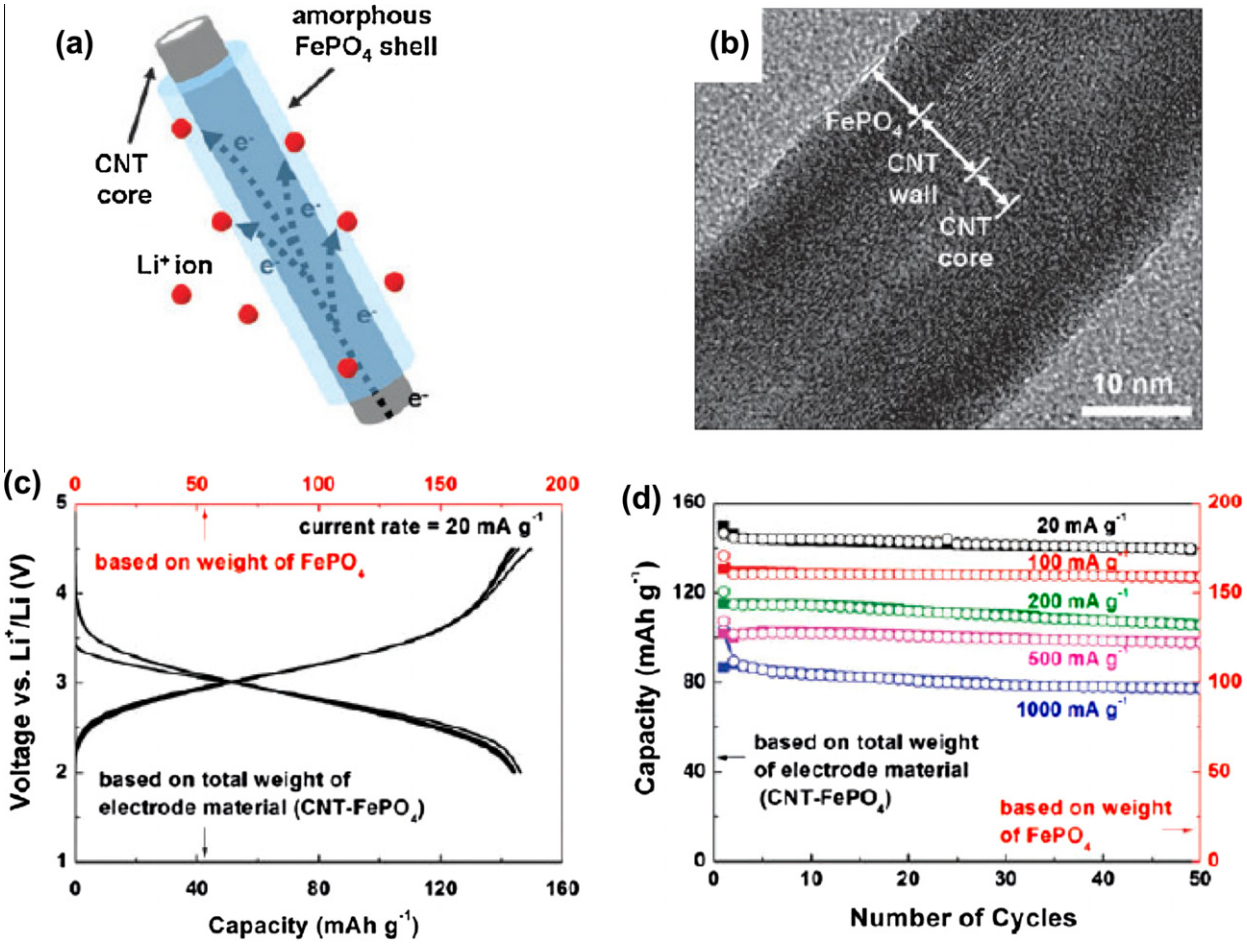

Fig. 9. (a) Schematic illustration of CNT-amorphous $FePO_4$ core–shell nanowire; (b) HRTEM image of core–shell nanowire; (c) charge–discharge profiles of the initial five cycles at a current rate of 20 mA g^{-1}; and (d) specific capacity as a function of number of cycles at current rates of 20, 100, 200, 500, and 1000 mA g^{-1}. After Kim et al. [62].

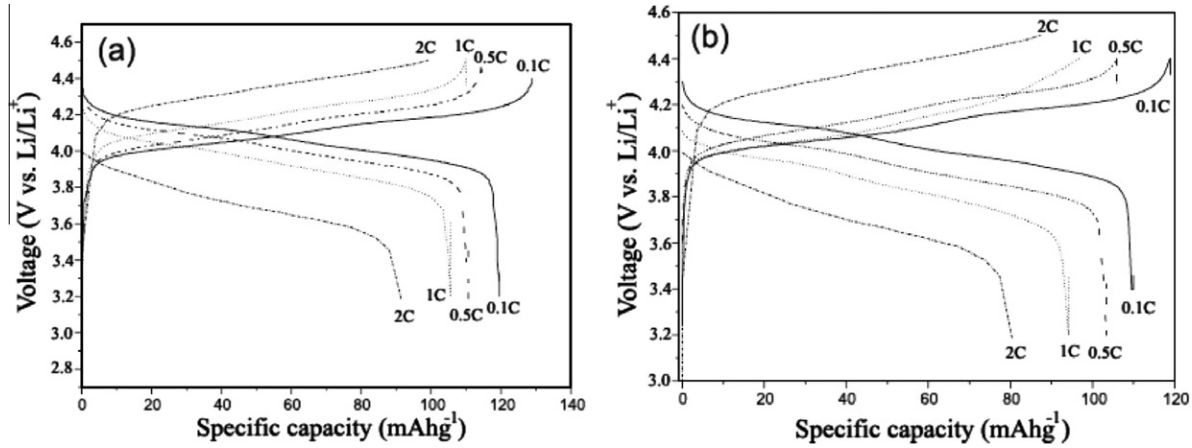

Fig. 10. Initial charge–discharge curves of the composites with (a) MWCNTs and (b) AB at different rates with the cutoff voltage between 3.2 and 4.3 V. After Liu et al. [63].

reduction in capacity was almost negligible along with a much higher initial discharge capacity of ~145 mA Hg^{-1} when MWCNTs were added into the cathode material. MWCNTs facilitated the formation of 3D networks that connected the $LiFePO_4$ particles, improving the transport characteristics of Li ions and electrons at high rates. It was also claimed that the expansion of citric acid during the charge–discharge process reduced the particle size, thus reducing the diffusion path, which in turn improved the reversibility of Li ion intercalation/extraction.

A high-rate capability is essential for future battery applications like electric vehicles that require a high power density during operation. The hierarchical nanostructure with $FePO_4$ shell directly grown on the CNT core was used as a cathode material for LIBs, which exhibited excellent electrochemical properties [62]. Fig. 9a schematically illustrates the core–shell structure of amorphous $FePO_4$/CNT hybrid nanowires, through which Li ions and electrons could readily diffuse into and out because of its nanometer scale and large surface area. It is expected that the improved transport

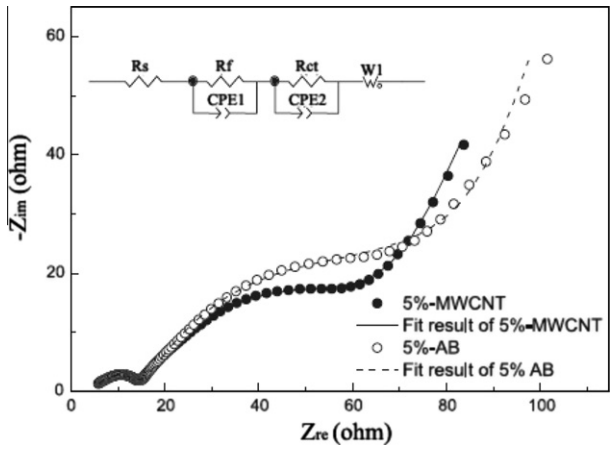

Fig. 11. Nyquist polts of $LiMn_2O_4$ composite cathodes containing 5 wt.% MWCNT and AB at room temperature (with equivalent circuit inert). After Liu et al. [63].

can enhance the rate capability of LIBs. The high resolution transmission electron microscopy (HRTEM) image in Fig. 9b clearly identifies the amorphous nature of the outer shell.

The charge–discharge curves of the initial five cycles of the core–shell electrode at a current rate of 20 mA g^{-1} are shown in Fig. 9c. The discharge capacity measured based on the total weight of the core–shell structured nanowire electrodes was about 149 mA Hg^{-1} at the first cycle and then it was reduced to 140 mA Hg^{-1} after several cycles with high reversibility. A clear potential plateau near 3.4 V was similar to the crystalline olivine $LiFePO_4$ cathode. This behavior has an advantage in monitoring the state of charge during battery operation. The specific capacities of the nanowires at different current rates are shown in Fig. 9d. The left and right *Y*-axes represent the specific capacities calculated based on the total weight of nanowires and the weight of amorphous $FePO_4$ shell alone, respectively. The high specific capacity of the nanowires was retained after 50 cycles even at high current rates up to 1000 mA g^{-1}. The reversible capacities were about 160, 133, 125 and 100 mA Hg^{-1} based on the weight of the amorphous $FePO_4$ shell at current rates of 100, 200, 500, and 1000 mA g^{-1}, respectively.

3.3. $LiMn_2O_4$/MWCNT nanocomposites

A few studies have also been reported for improving the electrochemical performance of $LiMn_2O_4$ electrodes by incorporating oxidized MWCNTs [63]. Fig. 10 presents the results from the galvanostatic charge–discharge tests of $LiMn_2O_4$/MWCNT cathodes. The initial discharge capacities were 119.4, 110.6, 105.5 and 91.4 mA Hg^{-1} at the rates of 0.1, 0.5, 1 and 2 C, respectively, which were much higher than the conventional $LiMn_2O_4$/AB with the same additive content. It was concluded that the improved conductive networks facilitated connection between the active materials and electron transport, with associated enhancements in rate capability and cyclic performance. Fig. 11 shows the electrochemical impedance spectra (EIS) of $LiMn_2O_4$ with MWCNTs or AB additives. The charge transfer resistance R_{ct}, a measure of electrochemical reactions at the electrode–electrolyte interface and particle-to-particle contact, was 34.32 and 53.2 Ω, respectively, for $LiMn_2O_4$/ox-MWCNT and $LiMn_2O_4$/AB composites, indicating a much lower charge transfer resistance of the former cathode material containing MWCNTs. The 3D networks formed by oxidized MWCNTs increased the contact area of active materials, effectively reducing the charge resistance.

$LiMn_2O_4$/MWCNT nanocomposites were also prepared by a facile sol–gel method [64]. The nanocomposites showed high cyclic performance with a remarkable capacity retention of 99% after 20 cycles, which is much better than the corresponding initial capacity loss of 9% after 20 cycles for the neat $LiMn_2O_4$ nanoparticles, as shown in Fig. 12a. Fig. 12b presents a significant reduction in charge transfer resistance from 120.4 Ω for the spinel $LiMn_2O_4$ to 98.3 Ω for the $LiMn_2O_4$/MWCNT nanocomposite, a direct reflection of the improved electrical conductivity arising from the intimate networking by MWCNTs among the spinel $LiMn_2O_4$ particles.

3.4. Intrinsically conducting polymer (ICP)/MWCNT nanocomposites

LIBs with cathode materials made from intrinsically conducting polymers (ICP), such as polyaniline (PANI), polyacetylene, polythiophene, polypyrrole and polymethylthiophene, have several important advantages over conventional LIBs with metal oxide cathodes, such as a longer cyclic life, a lower self-discharge rate, higher endurance to overdischarge, a lower manufacturing cost, more flexible shapes to form and easiness to make thin films. Among many conducting polymers, PANI is a promising candidate for the electrode material because it has good redox reversibility, high stability in air and aqueous solutions, and can be easily prepared using a chemical or electrochemical method at low production costs. However, the electrodes synthesized from conducting polymers also have problems related to stability, adherence and conductivity that may affect the reversibility of the electrode and thus limit their applications in energy storage devices. Recent studies have shown that the introduction of MWCNTs into PANI can en-

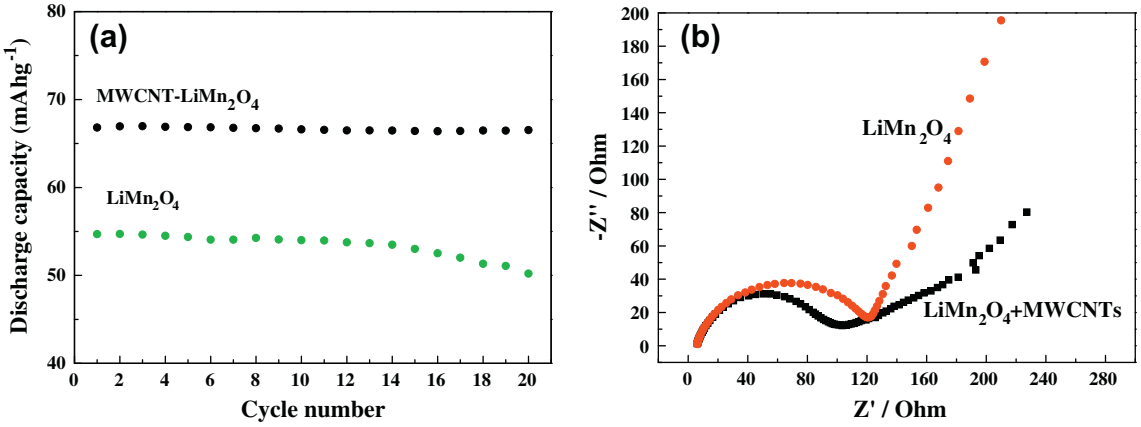

Fig. 12. (a) Residual discharge capacity of $LiMn_2O_4$ cathodes with and without MWCNTs versus cycle number at a rate of 2 C. (b) Impedance spectra of $LiMn_2O_4$ cathodes with and without MWCNTs.

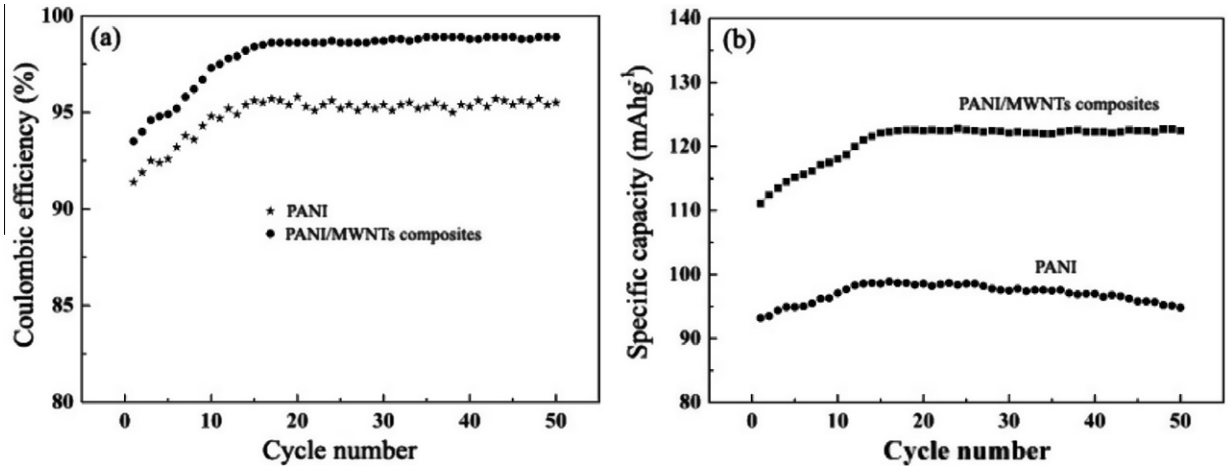

Fig. 13. Variations of (a) Coulombic efficiency and (b) discharge capacity of neat PANI and PANI/MWCNT composites as a function of cycle number from 2 to 4 V at a current density of 20 mA g^{-1}. After He et al. [68].

Table 4
Electrochemical performances of nanostructured cathode materials containing MWCNTs, CB, AB and CFs.

Electrode	Current rate	Initial discharge capacity (mA hg^{-1})	Cyclic performance (cycles)	Residual discharge capacity (mA hg^{-1})	Charge transfer resistance (Ω)	Ref.
LCO/MWCNT	2C	118	20	118	375	[52]
LCO/CF	2C	98	20	88.2	1000	[52]
LCO/CB	2C	86	20	60.2	5500	[52]
LCO/MWCNT	1C	144	40	119.5	10	[55]
LCO/CB	1C	146	40	99.3	20	[55]
LNC/CB	1C	169	50	138.6	90	[53]
LNC/MWCNT	1C	214	50	199.0	56	[54]
LFP/MWCNT	0.25C	138	30	142		[59]
LFP/CB	0.25C	135	30	132		[59]
LFP/MWCNT	0.1C	155	50	145.7	105	[60]
LFP/CB	0.1C	147	50	132.3	154	[60]
LFP/MWCNT	0.5C	145	50	151	76	[61]
LFP/CB	0.5C	112	50	123	115	[61]
LMO/AB	2C	80	40	72	53.2	[63]
LMO/MWCNT	2C	92	40	90	34.3	[63]
LMO	2C	54.7	20	49.8	120.4	[64]
LMO/MWCNT	2C	66.5	100	63.8	98.3	[64]
PANI	20 mA g^{-1}	94	50	99	154	[68]
PANI/MWCNT	20 mA g^{-1}	111	50	123	94	[68]

*C represents theoretical capacity of LCO, LNC, LFP and LMO, respectively.

hance the electrical properties by facilitating charge transfer processes between the two components [65–67]. An extremely high efficiency close to 100% with a discharge capacity of 120 mA Hg^{-1} was achieved using these composite electrodes along with Li metal and an ionic liquid electrolyte [65].

PANI/MWCNT composites prepared by an *in situ* chemical oxidative polymerization method were also extensively studied [68]. The charge transfer resistance of the electrode was reduced due to the incorporation of MWCNTs. Coulombic efficiency is an important index in assessing the performance of LIBs. An increase in Coulombic efficiency is often reflected by an increase in reversibility of charge–discharge cycle as the cycle number increases. As shown in Fig. 13a, the Coulombic efficiency approached 99% for the PANI/MWCNT composites and only about 95% for the neat PANI. The variations of discharge capacity with the cycle number for these materials are shown in Fig. 13b. The discharge capacity of the PANI/MWCNT composites (122.8 mA Hg^{-1}) was much higher than that (98.9 mA Hg^{-1}) of the neat PANI. The result remained much the same even after the neat PANI was applied in the form of nanofibers [69].

To summarize the above discussions, the relative electrochemical performances of the cathode materials containing different types of carbon materials, such as MWCNTs, CB, AB and CF, are tabulated in Table 4. It is clearly seen that both the initial and residual discharge capacities of the composite cathodes containing MWCNTs are significantly higher than those with other types of additives, CB, AB or CFs, regardless of the types of metal oxide materials. In addition, the corresponding charge transfer resistance was generally lower for the former than the latter cathode materials. The CNTs facilitated the formation of electric/thermal conductive networks that reduced the inner resistance and enhanced the thermal dissipation, ultimately resulting in higher specific capacities even at high charge–discharge current rates as well as enhanced safety for LIBs.

3.5. Other nanocomposites containing MWCNTs as conductive additive

Several other types of nanocomposite cathode materials have been synthesized using CNTs. For example, MWCNTs were coated with Co_3O_4 nanocomposites by a chemical precipitate method for

use as cathode material [70]. The capacities of the MWCNT/Co_3O_4 nanocomposite cathodes measured during Li insertion and extraction were 591.7 and 407.9 mA Hg^{-1}, respectively. These values are almost twice those of the MWCNTs used (313.7 and 217.6 mA Hg^{-1}, respectively), but were much lower than those of the Co_3O_4 cathodes (1100.5 and 682.7 mA Hg^{-1}, respectively).

PVC/CNT nanocomposites were synthesized via electrochemical polymerization of N-vinyl carbazole (VC) on CNT films, whose charge–discharge characteristics were evaluated [71]. After 20 cycles, high specific discharge capacities of 45 and 115 mA Hg^{-1} were obtained for PVC-functionalized SWCNTs and MWCNTs, respectively. This study provided two important pieces of information: namely (i) the hybrid nanocomposites can perform much better than the neat PVC for use as cathode material and (ii) the PVC/MWCNT nanocomposite presents a higher discharge capacity than the PVC/SWCNT nanocomposite.

The elemental materials to be used as positive electrode for LIBs should have an inherently high discharging capacity and an excellent cyclic life, along with long-term operation and a low cost. A Li/S redox couple has a theoretical specific capacity of 1672 mA Hg^{-1}, and a theoretical specific energy of 2600 W h kg^{-1}, based on sulfur active material and assuming complete reactions between Li and S to form Li_2S. Use of S is in general advantageous because it is environmentally benign and inexpensive. It also has disadvantages, such as a low conductivity and easy dissolution in the electrolyte to form polysulfide. MWCNTs were incorporated into sulfur to enhance the electrical conductivity and thus to reduce the dissolution of sulfur [72]. The initial discharge capacity of the sulfur electrode containing MWCNTs was 485 mA Hg^{-1} at 2.0 V *vs.* Li/Li^+. The cyclic life and rate capability of sulfur cathodes increased significantly as a result of adsorption of polysulfides by MWCNTs. In addition, the structural modification of the carbon matrix resulted in increases in both sulfur utilization and cyclic life of the Li/S batteries.

4. Anode materials

Considerable attention has recently been attracted to Li alloy materials containing elements such as Si, Al and Sn for application as negative electrodes of LIBs because these elements possess a higher theoretical specific capacity than that of the traditional anode material, graphite [73–76]. Among these, Si has the highest value. The practical use of Si particles, however, is significantly hindered because of two major problems. One is the low electrical conductivity and the other is the severe volume expansion/contraction during the alloying and de-alloying reactions with Li ions [77–80]. Several failure modes of Si particle electrodes have been identified [81,82]: Si particles expanded upon charging as a result of the alloying reaction, leading to swelling of the electrode layer, where carbon powder was also added to compensate for the poor conductivity of Si particles. In the following discharging period, the Si particles contracted as a result of the de-alloying reaction, but the electrode layer remained swollen because of its inelastic nature. The net result after the charge–discharge cycles was breakdown of the conductive networks that existed between Si, carbon particles and the current collector.

Several approaches have been proposed to address the above problems: for instance, breakdown of the conductive network can be minimized either by (i) applying a pressure on cells [83] using an elastomeric binder [84] or (ii) forming a composite with conductive materials, such as CNTs [85,86]. Different carbon additives show different degrees of crystallinity, morphology and particle sizes, which in turn influence the conductivity and electrolyte absorption capacity and thus the overall capacity of the cell. The large electrochemically accessible surface area of porous nanotube arrays and their high conductivities make them an ideal anode material for LIBs.

Apart from Si, intermetallic compounds, transitional-metal oxides (MO, where M is Co, Ni, Cu or Fe) and Sn/C nanostructured composites have also been studied, showing that they possessed high electrochemical capacities with 100% capacity retention for up to several hundred cycles and high recharging rates [87–91]. One of the disadvantages of these materials was that their synthetic routes were very complicated and expensive.

4.1. CNTs as anode materials

CNTs possess a unique shape and a high capacity that are useful characteristics for use in LIBs, particularly if Li ions can be intercalated into the tube. Template-synthesized CNTs can be fabricated as free-standing nanoporous carbon membranes, and narrower, highly ordered graphitic CNTs can be prepared within the membrane's tubules [92]. Both the outer and inner tubules are electrochemically active for intercalation of Li ions. Electrochemical test results showed that the CNT membrane electrodes exhibited a reversible intercalation capacity of 490 mA Hg^{-1}. The CNT structure and the degree of graphite crystallinity play a major role in determining both the specific capacity and cyclic life of CNT membranes [11–15,92,93]. The cycleability of highly-graphitized MWCNTs was more stable than that of slightly graphitized MWCNTs, whereas the slightly graphitized MWCNTs had a higher specific capacity than the highly-graphitized MWCNTs. This observation is attributed to the fact that Li tended to be doped preferentially into the regions with less organized graphitic structures, microcavities, edges of graphitic layers or the surface of single graphitic layers. Nevertheless, graphitized CNTs in general showed a higher capacity of Li intercalation than amorphous CNTs [94]. The electrochemical performance of CNTs during Li insertion correlates well with their micro-texture and chemical compositions that are affected by the synthesis conditions [94–96]. The rather discouraging results on Li insertion capability of MWCNTs in an earlier paper [97] further confirmed the importance of CNT structure.

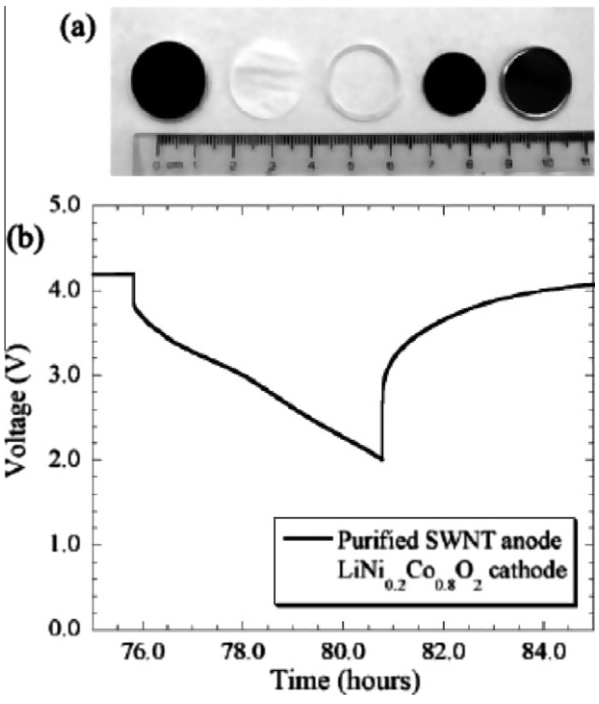

Fig. 14. Incorporation of SWCNTs into Li-ion batteries: (a) coin cell components and (b) discharge data for a coin cell containing a purified SWCNT anode and a $LiNi_{0.2}Co_{0.8}O_2$ cathode operating at 25 °C. After Raffaelle et al. [98].

Table 5
Effect of processing and material parameters on electrochemical performance of CNT anode materials.

MWCNT	The initial capacity (mA Hg^{-1})		Cyclic performance (cycles)	Residual capacity (mA Hg^{-1})		Ref.
	Charge	Discharge		Charge	Discharge	
Pristine	312					[99]
Chemically Etched	422	2087	100			[99]
Purified	351	641	50	311		[101]
Ball-milling			50	616		[101]
Short CNTs	502	1295	50		230	[104]
Long CNTs	188	615	50		142	[104]

Instead of using CNTs as the main anode material, studies have also been made on incorporation of CNTs as additive into the otherwise graphite dominant anode in anticipation to improve the capacity due to the CNT's higher electrical conductivity and specific surface area than graphite. The electrochemical performance of LIBs relies largely on the efficient cyclic insertion/extraction of Li ions between the cathode and anode, where rapid charging, high ionic storage and slow discharge constitute ideal device characteristics. Coin-cell batteries constructed using purified SWCNT 'paper' as the anode and $LiNi_{0.2}Co_{0.8}O_2$ as the cathode material were reported [98]. An overview of the components used to fabricate the battery is shown in Fig. 14a: they are from left to right (1) cathode mixture in aluminum cap, (2) Celgard separator, (3) O-ring, (4) SWCNT anode, and (5) stainless steel cell base. Fig. 14b shows the typical charge–discharge behavior for the SWCNT anode coin cell. The first discharge cycle had a capacity of 166 $mAhg^{-1}$ under these conditions, demonstrating the viability of SWCNT anode material.

4.2. Factors affecting performance of MWCNT anode materials

There are several important factors that affect the electrochemical performance of CNT anode materials, among which the surface condition and length of CNTs have been extensively studied. The MWCNTs were modified through chemical etching, ball-milling and shortening, and their influences on the initial and residual capacities are summarized in Table 5 and the details are discussed in the following.

A large number of defects and pores were introduced to MWCNTs as a result of chemical etching by HNO_3, which were correlated to enhancements of the capacity in the voltage range above 1.0 V and the reversible capacity [99,100]. These observations were related to preferential doping of Li ions onto the reactive defect sites rather than the perfect carbon structure. Although the ball-milling treatment also increased both the reversible capacity and Coulombic efficiency of MWCNTs, a large voltage hysteresis occurred because of the large amount of surface functional groups formed on MWCNTs [101]. The voltage hysteresis of MWCNTs was partly related to the kinetics of Li diffusion into the inner cores of MWCNTs, which could be reduced by cutting the MWCNTs into shorter segments [102].

Extensive research has been made to evaluate the effect of MWCNT length on the performance of anode material [103–105]. A new approach was developed to cut conventional micrometer-long entangled MWCNTs into about 200 nm long segments that could give rise to excellent dispersion. The reversible capacity of LIBs increased, whereas the irreversible capacity decreased upon shortening the MWCNT lengths because the insertion/extraction of Li ions into/from the short MWCNTs were easier than long MWCNTs. Moreover, short MWCNTs had a lower electrical resistance and Warburg prefactor, resulting in better rate performance at high current densities [103]. It can be seen from Fig. 15 that short MWCNTs had a higher Li extraction capacity than the long MWCNTs, and the specific capacities became stable after 30 cycles for both electrodes. The retention of reversible capacities after 50 cycles was also higher for short MWCNTs (77%) than long ones (60%).

A basically analogous conclusion has been drawn in another study on the effects of CNT type and length synthesized by two different methods [105]: short CNTs or carbon nanorods, a few hundred nm in length, were synthesized by oxidation and carbonization of carbon-encapsulated iron carbide/iron nanorods, whereas long CNTs, a few μm in length, were synthesized by catalytic pyrolysis of C_3H_6 using Fe as catalyst. The reversible capacities of the electrode made from short CNTs were 266 and 170 mA Hg^{-1} at current densities of 0.2 and 0.8 mA cm^{-1}, respectively, which

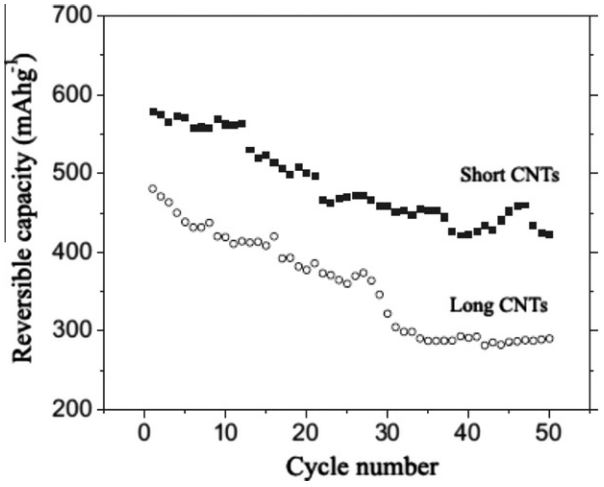

Fig. 15. Variation of Crev with number of cycles at a current density of 25 mA g^{-1}. After Wang et al. [103].

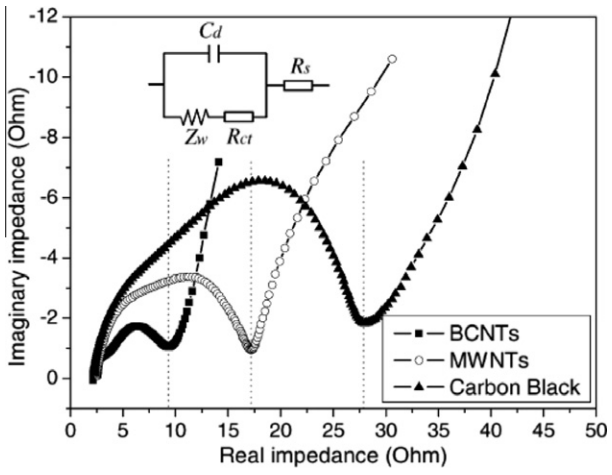

Fig. 16. Electrochemical impedance spectra of 5 wt.% BCNTs, straight MWNTs and carbon black in graphite anode materials. After Lv et al. [107].

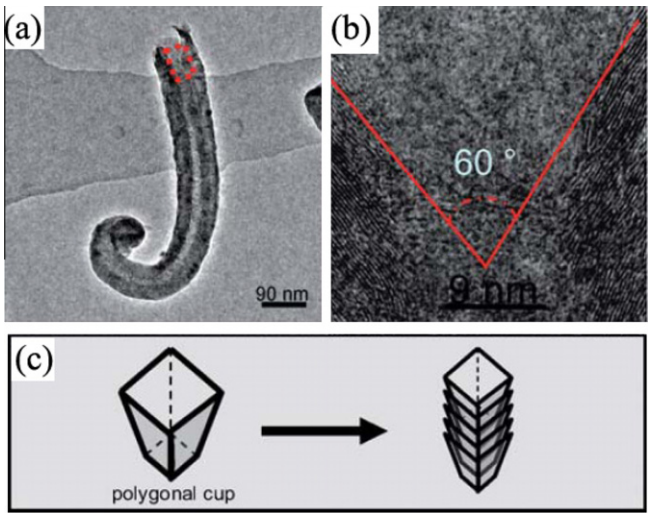

Fig. 17. (a) TEM image and (b) megascopic HRTEM image of the selected red area in image (a) of an as-prepared q-CNT, and (c) schematic structural model of polygonal cup-stacked-type. After Zhou et al. [108].

were almost twice those of the electrodes containing long CNTs. Both the surface film and charge-transfer resistances of the short CNTs were significantly lower than those of the long CNTs; and the Li diffusion coefficient of the electrodes made from both CNTs decreased with decreasing voltage, the reduction being more serious in long CNT electrodes than short ones. These observations further confirmed a higher electrochemical activity and more favorable kinetic properties during the charge–discharge process in the electrodes made from short CNTs.

Li ion insertion in MWCNTs occurs only in the low potential region and clearly differs from the case of graphite. While the typical discharge curve of the latter usually shows a staging phenomenon characterized by several potential plateaus, such a behavior is not observed in MWCNTs. Because of the morphological complexity of the CNTs, the identification of Li storage sites in general remains the main hindrance for elucidating the mechanism of Li insertion. Indeed, different from graphite, Li storage in CNTs is much more affected by the presence of so-called "3D defects", such as cavities and pores of different shapes and dimensions [106]. Therefore, unexpected results are often obtained when CNTs with unique structures are used as the anode material of LIBs.

As important members of the carbon nanotube family, bamboo-shaped carbon nanotubes (BCNTs) and quadrangular carbon nanotubes (q-CNTs) were thought to be suitable for anode material in LIBs, due to better improved cyclic stabilities and higher electric conductivity than common MWCNTs [107,108]. BCNTs that possess a high percentage of edge-plane sites on the surface exhibited better electrochemical characteristics with a faster electron transfer rate than their straight CNT counterparts with smoother and more basal plane regions. Fig. 16 presents the EIS of the BCNT, MWNT and CB samples. The significantly reduced resistance arose from the higher electron transfer kinetics of the BCNTs than those of CB and MWNTs due to the better wettability, more edge sites and more oxygen functional groups, and easier formation of 3D electrical conduction networks in BCNTs.

Novel q-CNTs were prepared on a large-scale production and investigated as the anode material for LIBs [108]. Compared with traditional CNTs, the q-CNTs possess a novel nanostructure, such as quadrangular cross section, one open end and "herringbone"-like walls, as shown in Fig. 17. The unique nanostructure of q-CNTs could shorten the diffusion time by both increasing diffusion coefficient and decreasing the diffusion pathway, resulting in an excellent rate capability.

Doping of CNTs using a heteroatom is also found to be efficient in improving the electrochemical performance of CNT anodes: boron- and nitrogen-doped MWCNTs as anode materials have been studied. Boron-doped MWCNTs exhibited a discharge capacity of 180 mA Hg^{-1}, which is higher than 156 mA Hg^{-1} for the undoped counterparts [109]. Prepared from pyridine as a precursor, nitrogen-doped MWCNTs were shown to have a reversible specific capacity of 340 mA Hg^{-1} [110]. The improved electrochemical performance is attributed to boron or nitrogen doping leading to a breakdown in in-plane hexagonal symmetry of CNT walls, resulting in an increase in electrical conductivity [111,112]. Composites are often the only way to maximize the performance of the constituent materials. A nanocomposite of CNTs and gold particles in a block copolymer matrix sustained more than 600 cycles at rates ranged from C/1.8 to 8.8C [113]. The composites had enhanced Li-ion diffusion through improved electronic conductivity.

MWCNTs are particularly attractive because they possess sites, where Li ions can be intercalated: spacing between the graphene layers, local turbostatic disorders arising from the highly defective structures, and the central core [92–96]. The large capacities are often ascribed to defects and shortened length of the nanotubes, which can improve Li diffusion properties [114]. Other advantages of MWCNTs, such as high electrical and thermal conductivities, endow MWCNT electrodes with high power outputs and good heat dissipation, improving the safety of the devices. One typical disadvantage of using CNT anodes is the irreversible capacity charge loss in the first cycle due to the SEI formation on the nanotubes that needs to be overcome during the battery charge phase. The other is the difficulty of uniform dispersion into the electrodes.

4.3. Nanocomposite anode materials containing CNTs as conductive additive

Previous studies have shown that the reversible capacity of CNTs varied widely depending on the synthesis method and treatment technique employed. The irreversible capacity, however, was too high to realize practical applicability. Furthermore, the reduction in capacity upon charge–discharge cycles was very high due to the detrimental surface reactions with solution species [115]. The formation of intense surface films may increase the electrode impedance and even electrically isolate part of the active mass [116]. In order to overcome these issues, several methods have been developed, including the use of MWCNTs as additive. Many different CNT composites with a variety of Li storage materials have been studied, such as Sn/MWCNT [117,118], Bi/MWCNT [119], SnSb/MWCNT [120,121], $CoSb_3$/MWCNT [122], $CoSn_3$/MWCNTs [123], Ag/Fe/Sn/MWCNT [124], TiO_2/MWCNT [125,126] and SnO_2/MWCNT [127,128] for use as anode materials. Li storage metals and metal oxides, such as Sn, Sb, TiO_2 and SnO_2, easily develop cracks during the charge–discharge process in spite of their significantly high electrochemical Li intercalation capacities. The breakdown of the electrode is a major cause of rapid degradation of their capacities as a consequence of the large specific volume change during the lithiation and de-lithiation reactions. The combining of MWCNTs that can hinder the agglomeration and enhance the electronic conductivity of the active materials is responsible for the enhanced cyclic performance. Table 6 summarizes the electrochemical parameters, such as initial charge and discharge capacities and residual reversible capacities, of various anode materials with and without CNT additives, undeniably confirming much enhanced cycle performance of the nanocomposites containing MWCNTs as compared to the neat anode materials. The details of the changes in electrochemical properties affected by the presence of CNTs are discussed in the following.

Table 6
Electrochemical parameters of anode materials consisting of various types of MWCNT-based nanocomposite.

Electrode type	Current rate	Initial charge capacity (mA Hg^{-1})	Initial discharge capacity (mA Hg^{-1})	Cycle number	Residual reversible capacity (mA Hg^{-1})	Charge transfer resistance (Ω)	Ref.
Sn/MWCNT	0.1 C	643	1590	40	627		[117]
Sn-MWCNT	50 mA g^{-1}		570	30	442	16.4	[118]
SnNi-MWCNT	50 mA g^{-1}		512	30	431	17.3	[118]
Bi/MWCNT	25 mA g^{-1}	308	570	50	315		[119]
Sb	50 mA g^{-1}	648	1023	30	115		[120]
$SnSb_{0.5}$	50 mA g^{-1}	726	951	30	171		[120]
Sb/MWCNT	50 mA g^{-1}	462	1266	30	287		[120]
$SnSb_{0.5}$/MWCNT	50 mA g^{-1}	518	1092	30	348		[120]
$CoSb_3$/MWCNT		312	915	30	265	7.2	[122]
Ag/Fe/Sn/MWNT	0.2 mA cm^{-2}	530		300	420		[124]
TiO_2	50 mA g^{-1}	52	287	75	21	123	[125]
TiO_2/MWCNT	50 mA g^{-1}	168	830	75	165	75	[125]
SnSb/MWCNT	50 mA g^{-1}	680	1408	50	480		[121]
Ag-	0.2 mA cm^{-2}	500	250	30	172	15.8	[126]
TiO_2/MWCNT	0.2 mA cm^{-2}			30	>400		[127]
SnO_2/MWCNT	37.2 mA cm^{-2}		728.3	40	126.4		[128]
SnO_2	37.2 mA cm^{-2}		665.1	40	505.9		[128]
SnO_2/MWCNT	850 mA g^{-1}	100	100			60	[129]
$Li_4Ti_5O_{12}$	850 mA g^{-1}	145	145	500	142	38	[129]
$Li_4Ti_5O_{12}$/MWCN	50 mA g^{-1}		819	50	279		[147]
Si/MWCNT (7:3)	50 mA g^{-1}		1770	50	1250		[147]
Si/MWCNT (5:5)	50 mA g^{-1}		1182	50	889		[147]
Si/MWCNT (3:7)	0.25 mA cm^{-2}	960	1882	30	1066		[151]

*C is the theoretical capacity of Sn.

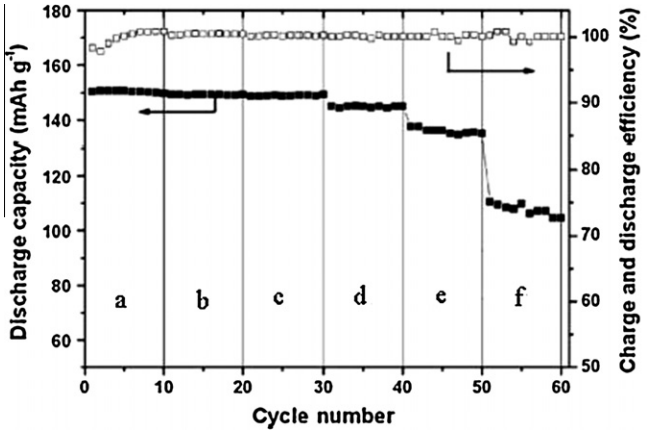

Fig. 18. Discharge capacity and charge–discharge efficiency versus cycle number for $Li_4Ti_5O_{12}$/MWCNT electrode at different rates of (a) 85 mA g^{-1}, (b) 170 mA g^{-1}, (c) 340 mA g^{-1}, (d) 850 mA g^{-1}, (e) 1700 mA g^{-1}, and (f) 3400 mA g^{-1}. After Huang and Jiang [129].

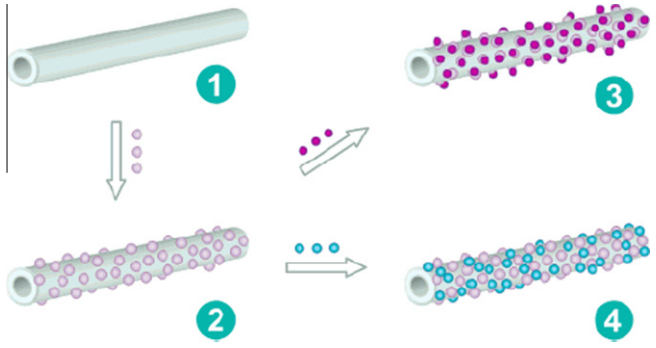

Fig. 19. Schematic illustrations of self-assembly for preparation of nanocomposites: (1) MWCNT as primary support; (2) a second phase of nanoparticles (in pink) are anchored onto MWCNTs, (3) a third phase of nanoparticles (in purple) are attached to the surface of the second phase nanoparticles, and (4) a third phase of nanoparticles (in blue) are also landed onto the MWCNTs. Further addition of phases can also be carried out with the same assembling strategy. After Li et al. [133]. (For interpretation of the references to color in this figure legend, the reader is referred to the web version of this article.)

4.3.1. $Li_4Ti_5O_{12}$/MWCNT composites

Spinel $Li_4Ti_5O_{12}$ has long been considered as a promising alternative to graphite anode material for LIBs. The combination of zero strain insertion properties and high Li mobility makes it an ideal anode material. However, its rate performance is severely limited due to its low electronic conductivity. The introduction of MWCNTs into $Li_4Ti_5O_{12}$ particles showed an ameliorating effect on rate capability and capacity retention [129]. The charge transfer resistance of $Li_4Ti_5O_{12}$ and $Li_4Ti_5O_{12}$/MWCNT electrodes was 60 and 38 Ω, respectively. The cycling stability of $Li_4Ti_5O_{12}$/MWCNT composite shown in Fig. 18 indicates that the discharge capacity was quite stable during the charge–discharge process at low current rates. Even after 500 cycles at 850 mA g^{-1} the discharge capacity was standing at 142 mA Hg^{-1}, which was 97.9% of the initial discharge capacity. It is worth noting that the anode could be charged at an extremely high rate of 3400 mA g^{-1}. These results confirmed that the $Li_4Ti_5O_{12}$/MWCNT composite electrode had a high rate capability and capacity retention, which can be attributed to the improvement in conductivity and the smaller size of $Li_4Ti_5O_{12}$ crystals in the $Li_4Ti_5O_{12}$/MWCNT composite electrode.

4.3.2. Transitional metal oxide/MWCNT composites

It is proven that transitional metal oxides could deliver reversible capacities as high as 1000 mA Hg^{-1} [130–132]. However, their applicability is limited by the large hysteresis in their charge–discharge curves and the relatively low electronic conductivity. Nanocomposites containing CNTs for energy storage applications are prepared by simply mixing MWCNTs with the functional metal or metal oxide particles based on various techniques. The resultant composites have a compositional variation across the radial direction and a constant concentric arrangement of each participating component along the axial direction, resembling an electric cable

configuration. A general approach to produce MWCNT/metal oxide nanocomposites via self-assembly was developed recently [133]. Schematic illustrations of the self-assembly of MWCNT nanocomposites are shown in Fig. 19. The self-assembly technique allows preparation of binary composites as well as more complex systems, such as ternary and quaternary composites. The nanoparticles of active phase, e.g., metals and metal oxides, serve as the primary building block to form various types of composites, including TiO_2/MWCNT, Co_3O_4/MWCNT, TiO_2/Co_3O_4/MWCNT and $Co/CoO/Co_3O_4$/MWCNT. It was shown that the self-assembled TiO_2/MWCNT composites were sufficiently robust and their electrochemical performance was significantly enhanced compared to neat TiO_2.

1D nanostructured electrode materials showed strong potential for LIBs due to their good electrochemical performance. Co_3O_4/CNT composites were synthesized using a hydrothermal method as anode material [134]. Nanocrystalline Co_3O_4/CNT composite anodes exhibited a reversible Li storage capacity of 510 mA Hg^{-1} over 50 cycles. Fe_3O_4/CNTs composites were also studied as anode material [135]. Fe_3O_4 nanoparticles were attached onto the sidewalls of modified CNTs by chemical coprecipitation of Fe^{2+} and Fe^{3+} in an alkaline solution. The electrochemical test results indicate that the initial discharge and charge capacities of the 66.7 wt.% Fe_3O_4/CNTs nanocomposite electrodes were 988 mA Hg^{-1} and 661 mA Hg^{-1}, respectively. The charge capacity retained after 145 cycles was 645 mA Hg^{-1}, which outperforms that of commercial graphite materials. The excellent cycleability and the high capacity retention of the electrodes are attributed to the framework of CNTs and deposition of nanosized Fe_3O_4 particles onto CNTs.

Incorporation of CNTs as an additive to active anode materials is an effective strategy to form conductive networks in the electrode at a content much lower than other carbonaceous materials, like carbon black and graphite. Many applications including aerospace, transportation and portable electronics require lighter weight and longer life batteries for electrochemical energy storage [136], which in turn depend on the weight and volume of the electrode, except for its energy content. New techniques have been developed to meet this requirement. CNTs have the capability to be assembled into free-standing electrodes as an active Li-ion storage material or as a physical support for ultra-high capacity anode materials like silicon or germanium [137]. The major advantage arising from utilizing free-standing CNT anodes is the removal of the copper current collectors, which can translate into an increase

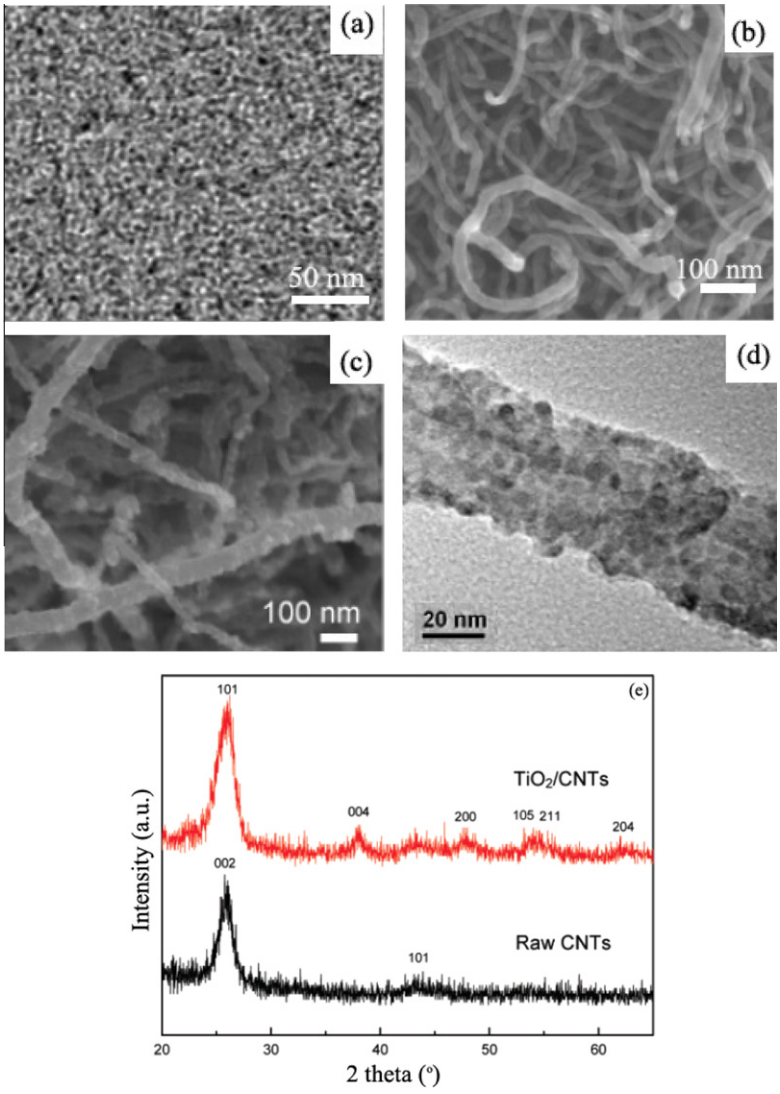

Fig. 20. (a) As-synthesized TiO_2 nanoparticles (TEM image), (b) raw MWCNTs (FESEM image), (c) as-prepared TiO_2/MWCNT nanocomposite (FESEM image), (d) magnified view of TiO_2/MWCNT nanocomposite (TEM images), and (e) XRD spectra of as-prepared TiO_2/MWCNT nanocomposite and as-received MWCNT. After Li et al. [133].

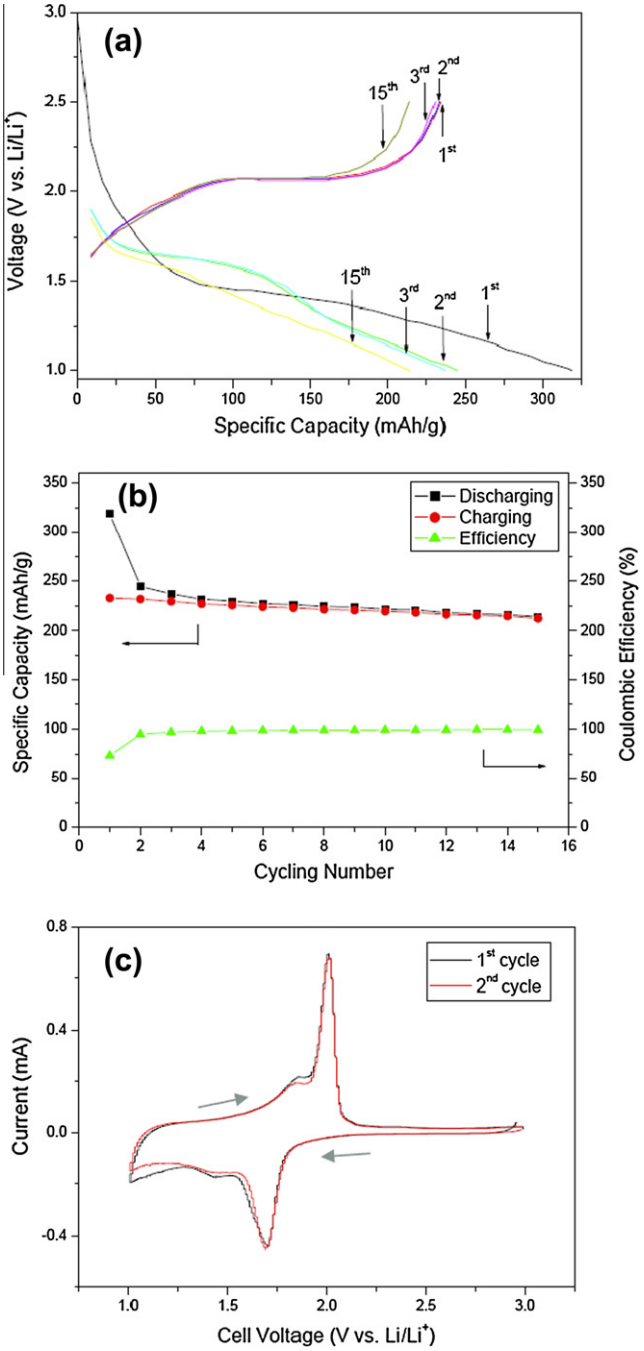

Fig. 21. Electrochemical properties of TiO_2/MWCNT nanocomposite anodes: (a) voltage profiles for discharging and charging cycles; (b) cyclic performance; and (c) cyclic voltammograms. After Li et al. [133].

in specific energy density by more than 50% for the overall battery design. However, major challenges, such as the first cycle charge loss and paper crystallinity for free-standing CNT electrodes, need to be overcome through further research.

4.3.3. TiO_2/MWCNTs nanocomposites

Fig. 20 shows representative images of the TiO_2/MWCNT nanocomposites and their starting building blocks. The as-prepared TiO_2 nanoparticles used in the composites had a narrow size distribution of 3–4 nm. The MWCNT nanocomposite exhibited a rough surface after decoration with uniformly dispersed TiO_2 nanoparticles (Fig. 20c and d). The corresponding XRD spectra (Fig. 20e) indicate that although the (101) diffraction of the metal oxide phase overlaps with (002) of MWCNTs, the TiO_2 nanoparticles maintain their pristine phase even after decoration onto the MWCNTs. All diffraction peaks can be indexed to tetragonal anatase TiO_2 nanorods (JCPDS file No. 21-1272).

The performance of the TiO_2/MWCNT system was tested in real working environments for LIB applications. To increase the electronic conductivity of anode materials, carbon black are normally mixed with the host material. However, a simple mechanical mixing cannot provide a uniform mixture, causing general problems like polarization of the active component and high resistance to electron transfer. When MWCNTs are evenly distributed between the active TiO_2 nanoparticles, the TiO_2/MWCNT nanocomposites may solve these problems. Although MWCNTs could serve as the major anode material, their discharge only occur at a potential of about 0–0.2 V (vs. Li/Li^+) [138,139] that is much lower than the limit of 1.0 V in this particular study. Therefore, it was assumed that the MWCNTs in the as-prepared TiO_2/MWCNT nanocomposites did not participate in the charge–discharge reactions, and acted only as oxide carrier and charge conductor.

Fig. 21a shows the charge–discharge profiles cycled between 1 and 2.5 V at a constant current density of 300 mA g^{-1}. Except for an irreversible reaction taking place in the first discharge cycle, both the discharge and charge curves for the 15th cycle show a profile much the same as the 2nd and 3rd curves with only a negligible shift. This implies that a stable structure was formed during the first Li insertion to the anatase TiO_2 nanoparticles. The cyclic performance of the TiO_2/MWCNT electrode shown in Fig. 21b indicates that the first specific discharge capacity was as high as 318.5 mA Hg^{-1} with a corresponding charge capacity of 233.0 mA Hg^{-1}. A drop of 26.8% was observed. However, from the 3rd to 15th cycle and onwards, the specific capacity showed only a marginal reduction, and the Coulombic efficiency (i.e., the ratio of Li extraction to Li intercalation capacity) was close to unity (>98%), indicating an excellent cyclic stability. The reversible capacity maintained stably during these cycles was about 225 mA Hg^{-1}, which is approximately 17% higher than the capacity of hydrogen titanate nanowires (~191.8 mA Hg^{-1}) [140], 32% higher than that of nanosized rutile TiO_2 (~170 mA Hg^{-1}) [141] or 50% higher than that of anatase TiO_2 (~150 mA Hg^{-1}) [142]. Fig. 21c presents two cycles of CVs at a slow sweep rate of 0.05 mV s^{-1}, further confirming the quasi-reversible process. Both CVs were recorded after 15 charge–discharge cycles, and they were relatively stable and showed nearly the same peak positions. These observations are testament to kinetically reversible Li ion intercalation into and extraction from the well-dispersed, uniform-sized TiO_2 nanoparticles and excellent electrochemical performance of the TiO_2/MWCNT system.

To increase the ionic and electronic diffusion and thus to achieve a high rate capability, unique nano-architectures were synthesized and electronically conductive phases were introduced into the nanocomposite. Nanocomposites consisting of brookite TiO_2 nanoparticles attached to MWCNTs [143] were also investigated as the anode materials for LIBs. Brookite TiO_2 crystallizes in the orthorhombic system which is different from the anatase and rutile forms of TiO_2 discussed in Section 4.3.2. The brookite crystallites had an average diameter of 7 nm, which was smaller than those obtained from pure brookite due to the homogeneous nucleation onto the MWCNT surface. Fig. 22 shows that the brookite/MWCNT composite gave rise to a remarkably high capacity and stable cycleability, useful attributes for anode materials in LIBs. The composites exhibited a high discharge capacity of 151 mA Hg^{-1} even after 100 cycles at a rate of C/5 (Fig. 22a). The beneficial effect of MWCNTs in the composite electrode was further evidenced by the large difference in charge–discharge profiles between the neat brookite and brookite/MWCNT composites

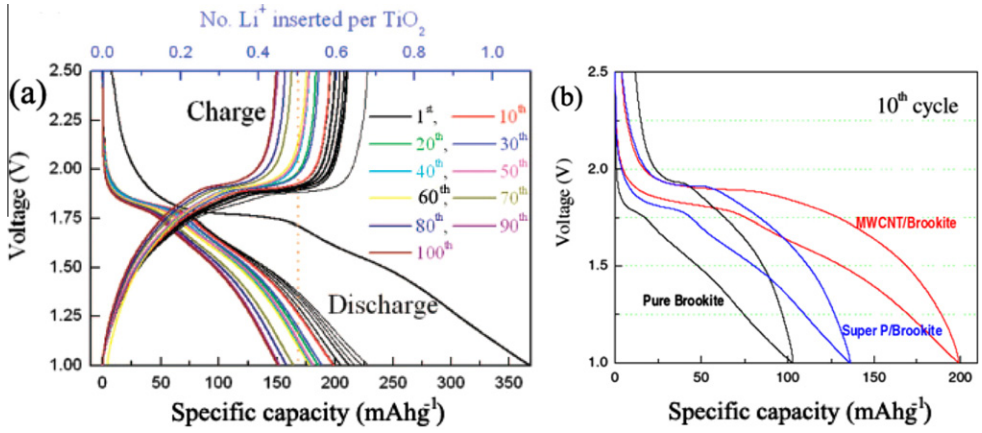

Fig. 22. (a) Charge–discharge curves (every 10th cycles) of brookite/MWCNT nanocomposite anodes cycled between 2.5 and 1.0 V at a rate of *C*/5; (b) comparison of cycling behaviors at the 10th cycle between neat brookite and brookite/MWCNT nanocomposite. After Lee et al. [143].

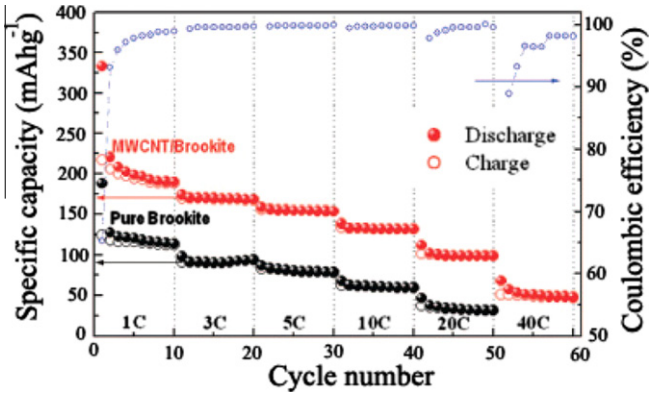

Fig. 23. Rate capability and Coulombic efficiency for neat brookite and brookite/MWCNT nanocomposite at different *C* rates. After Lee et al. [143].

(Fig. 22b). The reversible capacity was higher and the cell polarization was lower in the descending order of brookite/MWCNT, brookite/Super P and neat brookite. The 1D nature of MWCNTs offered well-developed conductive pathways between the active brookite particles and the copper current collector. The rate capacities and Coulombic efficiency of the brookite/MWCNT nanocomposites were much better than the corresponding values of the neat brookite under the identical conditions, as shown in Fig. 23. At rates of 3, 10, 20, and 40 C, the composites delivered specific capacities of 170, 132, 100, and 51 mA Hg^{-1}, respectively, maintaining an excellent Coulombic efficiency of higher than 98%. The MWCNTs facilitated rapid Li ion transport through the large electrode–electrolyte contact area.

Recently, well-organized CNT/TiO_2 core/porous-sheath coaxial nanocables were synthesized by controlled hydrolysis of tetrabutyl titanate in the presence of CNTs as anode material for LIBs [144]. The morphology of the CNTs was well maintained even after calcination, although their surface became slightly rough (Fig. 24a). A uniform sheath with a thickness of about 25 nm can be clearly seen from the image. The 0.34 nm spacing observed in the core of the coaxial nanocable corresponds to the (002) crystalline planes of the MWCNTs (inset in Fig. 24b). Lattice fringes with a spacing of 0.35 nm are clearly visible from the HRTEM image taken from the nanocable edge (Fig. 24c), which is in good agreement with the spacing of the (101) planes of anatase TiO_2, thus demonstrating the presence of nanocrystalline TiO_2.

Compared with neat CNTs or neat TiO_2, the CNT/TiO_2 coaxial nanocables showed a much improved rate capability and cycle performance. As shown in Fig. 24d, both the specific capacities of the CNT core and the TiO_2 sheath were much higher than that of the TiO_2-free CNT or that of the CNT-free TiO_2 sample. In addition, the capacity retention and the Coulombic efficiency kept almost 100% (Fig. 24e). It is thought that the coaxial cable morphology provides an ideal solution to the ionic-electronic wiring problem in LIBs as well as the synergism of the two cable wall materials. The storage of TiO_2 was improved by the contact with CNTs and, even more remarkably, the storage in CNT was improved by the presence of TiO_2.

New nano-sized TiO_2 rutile has been used as active material in LIBs. MWCNTs were added into the slurry formulation to partly replace Super P and the resulting electrodes were electrochemically characterized [58]. Fig. 25 shows the rate capability of TiO_2 rutile-based composite electrodes containing Super P as unique conductive agent and a Super P + MWCNTs combination at different current rates. The 1 wt.% MWCNTs in TiO_2 rutile-based anodes was efficient in enhancing the rate capability when the electrodes were cycled in the potential range 1.0–3.0 V, as well as increasing both the energy and power densities of LIBs.

4.3.4. SnO_2/MWCNT nanocomposites

SnO_2 has received much attention as an alternative anode material due to its high specific capacity of 782 mA Hg^{-1}. However, it experiences a large volume expansion of 260% during the charge–discharge cycles [145] and the incorporation of CNTs is one of the most well-established methods to reduce the volume expansion as well as to improve the electronic conductivity of the electrodes [127,128]. Instead of randomly mixing the active SnO_2 particles with CNTs, a new technique was developed to synthesize a co-axial SnO_2 tube/CNT nanostructure [146]. The porous SnO_2 nanotubes were formed first, and a uniform CNT overlayer was grown on the external surface of the SnO_2 nanotubes through a confined-space catalytic deposition process. The coaxial nanostructure delivered a reversible capacity higher than that of CNTs in the voltage window of 5 mV–3 V at a current rate of 0.5 C, as shown in Fig. 26. The capacity retention of 92.5% after 200 cycles is deemed similar to the performance of commercial graphite anodes. The outstanding electrochemical properties are likely to be related to several unique features of the nanocomposite: (i) tubular organization of SnO_2 nanoparticles, (ii) stress absorption by the CNT matrix, and (iii) the existence of a hollow interior allowing freedom of expansion, increased electrical contact, and enhanced Li-ion transport.

A novel mesoporous-nanotube hybrid composite was prepared by a simple method that involved *in situ* growth of mesoporous

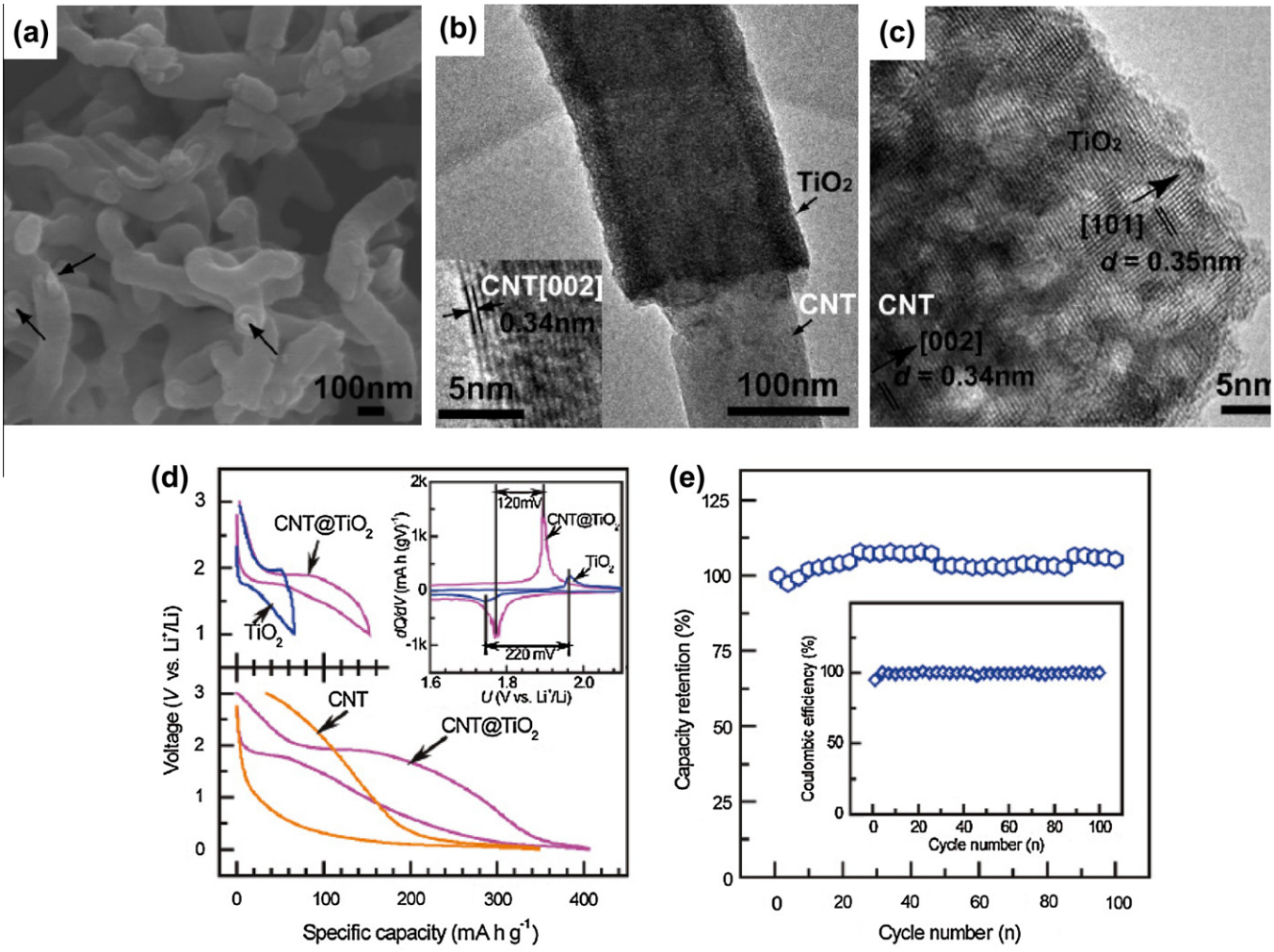

Fig. 24. (a) SEM images of CNT/TiO_2 coaxial nanocables; (b) and (c) HRTEM photographs of CNT/TiO_2 coaxial nanocables; (d) Typical discharge–charge profiles of CNT/TiO_2 nanocables, TiO_2-free CNT, and CNT-free TiO_2 electrodes at 50 mA g^{-1} between voltage ranges of 1–3 and 0.01–3 V, the inset shows the corresponding differential capacity plots; (e) cyclic performance of CNT/TiO_2 nanocables at 1000 mA g^{-1} in the voltage range of 0.01–3 V, the inset shows the corresponding Coulombic efficiency profiles. After Cao et al. [144].

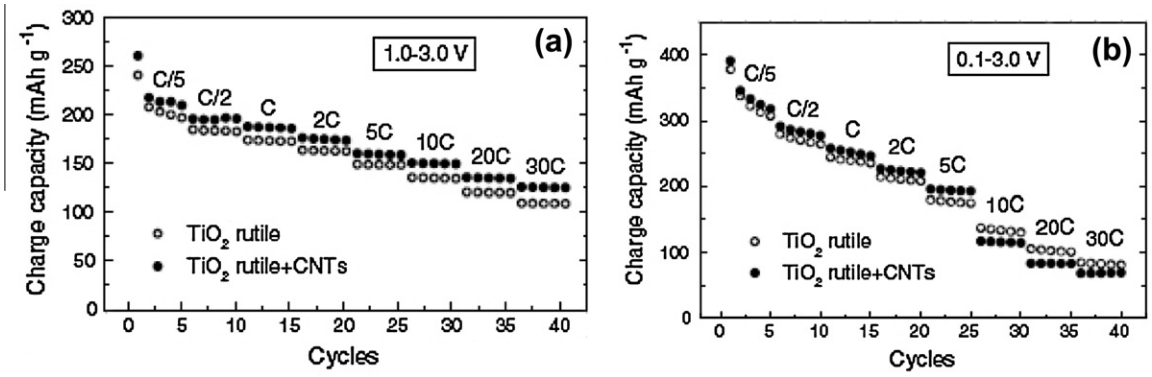

Fig. 25. Rate capability of TiO_2 rutile-based anodes in a $LiPF_6$ electrolyte at two different voltage windows: (a) 1.0–3.0 V and (b) 0.1–3.0 V. After Varzi et al. [58].

SnO_2 on the surface of MWCNTs through a hydrothermal method [147]. The electrochemical test results indicate that the mesoporous-tube hybrid composites displayed a higher capacity and better cycle performance than the neat mesoporous SnO_2, as shown in Fig. 27. The improvement was attributed to the synergistic effects of favorable properties, including the 1D hollow structure, high strength with flexibility, excellent electric conductivity and large surface area, which in turn facilitated the reduction in volume expansion, shortened Li ion diffusion path, easy transmission of electrons and stable structure after long cycles.

Other conducting elements are often added into the otherwise two-component SnO_2/CNT composite anodes. For example, 1D hy-

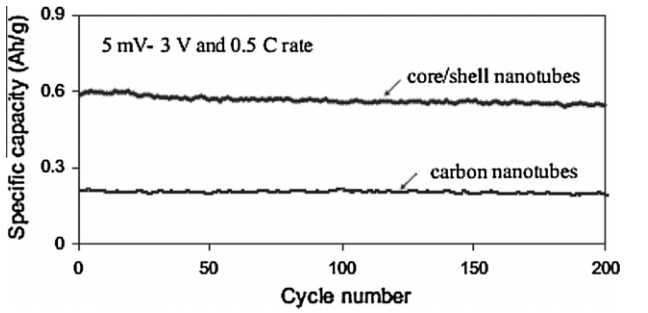

Fig. 26. Cyclic performance of SnO_2-core/carbon-shell nanotubes and CNTs at a current rate of 0.5 C and 5 mV–3 V (vs. Li^+/Li) voltage window. After Wang et al. [146].

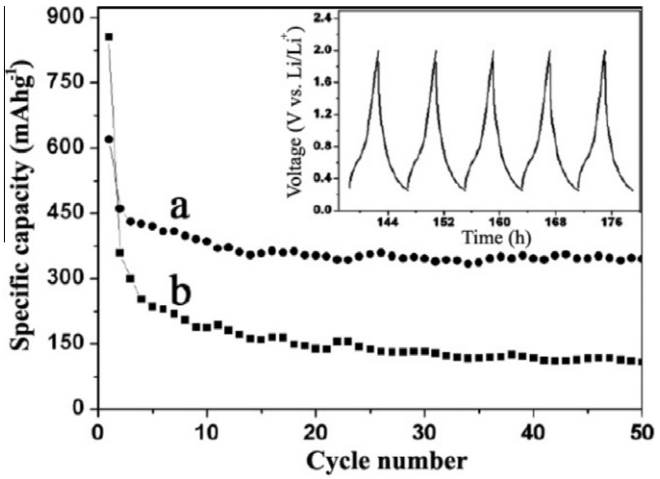

Fig. 27. Cyclic performance of (a) mesoporous SnO_2/MWCNT and (b) neat mesoporous SnO_2 measured at a current density of 33.3 mA g^{-1}. Inset shows the voltage-capacity profiles of the 16th–20th charge–discharge cycles of (a). After Wen et al. [147].

brid nanocables of Au–SnO_2/MWCNTs have been developed using a facile one-pot route and their electrochemical performance was studied [148]. The introduction of a small amount (0.9 wt.%) of Au species enhanced the conductive properties. Fig. 28a displays the XRD pattern of the Au-SnO_2/MWCNT nanocables confirming their crystallographic structure. The peak positions at 33.9 and 51.8° were assigned to tetragonal rutile SnO_2 (JCPDS Card No. 41-1445). However, the diffraction peaks corresponding to Au were not found. The TEM images (Figs. 28b) present that the MWCNTs were coated with a Au–SnO_2 hybrid layer of uniform thickness about 10–15 nm, forming nanocables of a diameter about 30–50 nm. The grain size of the coating material was very small and no lattice fringe was observed. Fig. 28c shows the rate performance of SnO_2/MWCNT nanocables with and without Au for rates up to 7.2 Ag^{-1}. The nanocables containing Au exhibited higher reversible capacities both at low and high rates than those without. The former nanocables with Au had stable reversible capacities of 467 and 392 mA Hg^{-1} at rates of 3.6 and 7.2 Ag^{-1}, respectively, corresponding to 62% and 52% of the capacities obtained at 0.18 Ag^{-1}. In contrast, the capacities were reduced to 370 mA Hg^{-1} (3.6 Ag^{-1}) and 242 mA Hg^{-1} (7.2 Ag^{-1}) for the nanocomposites without Au, corresponding to 60% and 39% of the capacities at 0.18 Ag^{-1}, respectively. The existence of Au species in the coating and the unique 1D architecture of CNTs as the template were mainly responsible for the enhanced reversible capacities of Au–SnO_2/MWCNT nanocables.

The Au-SnO_2/MWCNT nanocables had much lower charge transfer resistance in the medium frequency range than for the SnO_2/MWCNT nanocables, as shown in Fig. 29. The faradic reaction is determined by ion transfer and electron conduction indicating that the reduction in charge transfer resistance was likely attributed to the improved electronic conductivity of Au–SnO_2/MWCNT electrodes arising from the Au nanoparticles. Au, an excellent electronic conductor, helped improve the Li ion insertion/extraction reversibility as well as reduce the cell polarization. On the other hand, the hybrid nanostructure enhanced the electrolyte/SnO_2 contact area, shortened the Li ion diffusion path in the SnO_2 coating layer, as well as accommodated the strains induced by the volume change occurring during the electrochemical reactions. Another material that has been studied recently along with the SnO_2/CNT composite anodes is graphene or graphene oxide. Incorporation of 2D graphene sheets to form SnO_2/CNT/graphene hybrid composites in the form of powder or paper further improved the specific capacity as well as the cyclic performance due to the increased surface area and pore volumes [149].

4.3.5. Si/MWCNT nanocomposites

Silicon is one of the most attractive and widely investigated candidate anode materials due to its high theoretical specific capacity of 4200 mA Hg^{-1} corresponding to the fully lithiated composition of $Li_{4.4}Si$, which is 10-fold higher than that of graphite [75]. However, large crystallographic volume changes and several phase transitions occur during the Li insertion and extraction processes, leading to the generation of large mechanical strains. These strains cause cracking and breakdown of the electrode, which results in the failure of the anode after only a few cycles due to the loss of electronic contacts between the active particles [150].

In an attempt to improve the cycleability of Si-based anodes, second phase components have been introduced to serve as buffer so that a large volume change during cycling can be accommodated. Si/MWCNT nanocomposites with a unique core/shell structure [151] were fabricated, which showed superior anodic performance to that observed in electrodes made from bare Si or Si/MWCNT mixture. The results shown in Fig. 30 indicate that the specific capacities of the composites with a core/shell structure were at least twice higher than the other materials. It was proposed that the void space and the flexible characteristics in MWCNT buffer layer on the Si surface allowed volume expansion of Si core without severe electrode swelling. The electronic conductive networks formed by MWCNTs also helped reduce the charge transfer resistance. The relatively poor performance of the Si/MWCNT mixture compared to that with a core/shell structure suggests that the composites with active particles of intimate contacts is more advantageous than simple mixing.

The concept behind the enhanced electrochemical performance by the Si/CNT composites with a core/shell structure is illustrated schematically in Fig. 31, which is compared with the Si powder electrodes consisting of a random mixture of Si particles and CB. The electric conductive networks are easily broken during cycling of the conventional anode material because the Si particles tend to be debonded and separated from the binder after discharging (Fig. 31a). Once the CNTs are fully integrated with the Si particles to form a core/shell structure, the composite electrode can deliver much better electrochemical performance (Fig. 31b). The CNT layer can accommodate the volume expansion of core Si particles to minimize the electrode swelling. As a result, the electrical conductive network is maintained even after a large volume change in Si particles. The performance of the electrode made from a Si/CNT simple mixture was not equally improved (Fig. 31b) because the CNTs played essentially the same role as the CB.

Si/MWCNT composites with different weight ratios were produced using purified MWCNTs and Si powder through high-energy

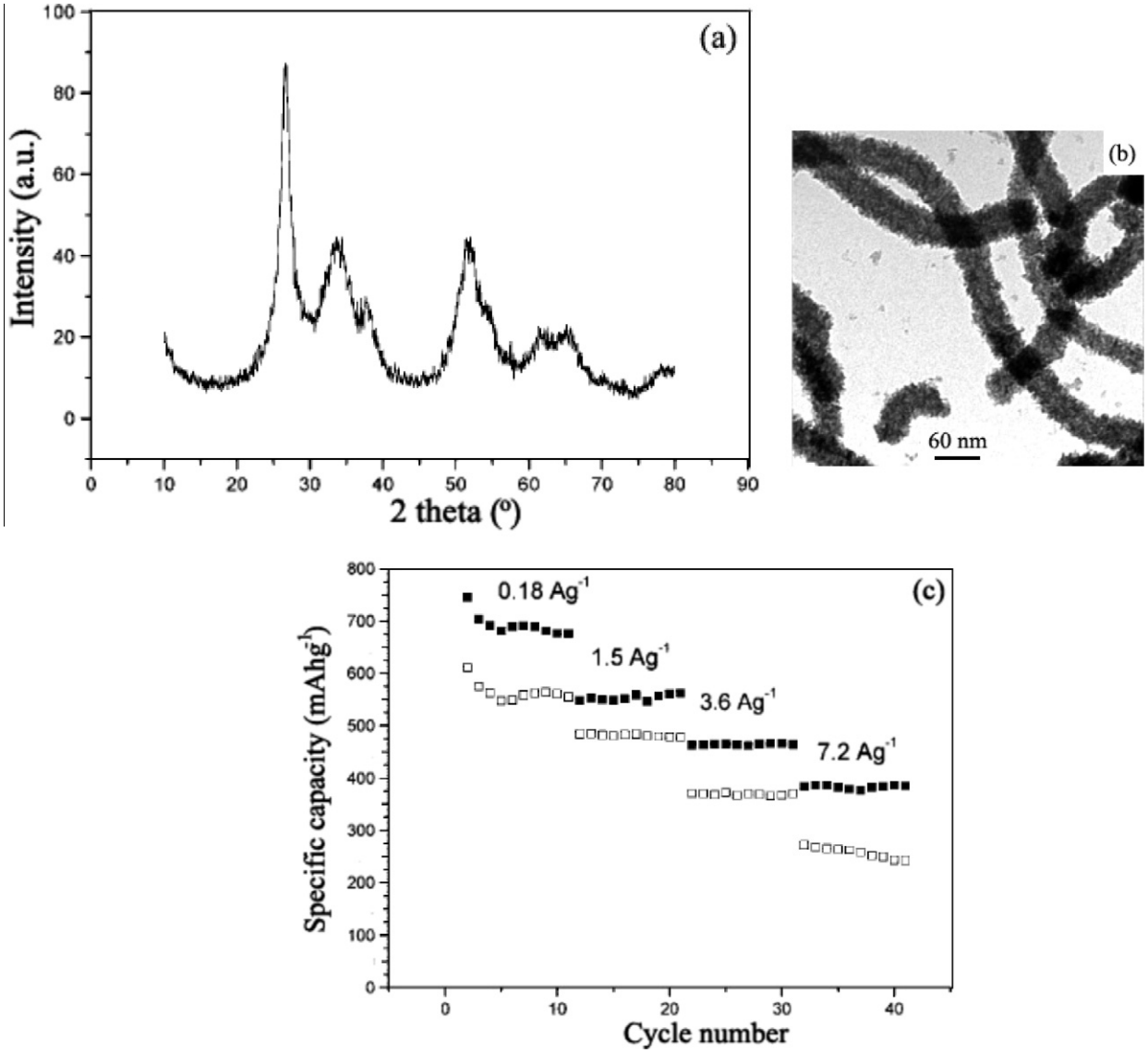

Fig. 28. (a) XRD spectrum for Au-SnO_2/MWCNT nanocable; (b) TEM images of Au–SnO_2/MWCNT nanocables; (c) discharge capacity vs cycle number for SnO_2–Au/MWCNT (■) and SnO_2/MWCNT (□) composites at different rates between voltage limits of 0.01 and 1.2 V. After Chen et al. [148].

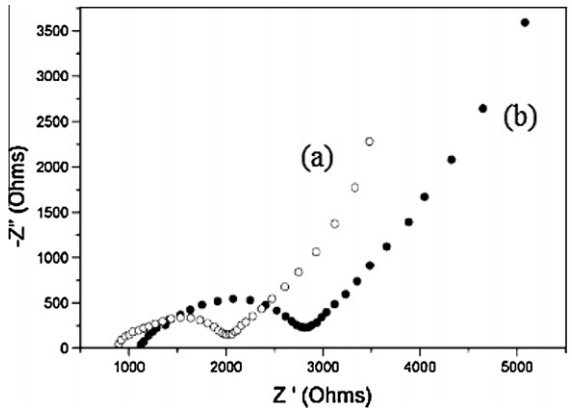

Fig. 29. Impedance spectra of (a) SnO_2–Au/MWCNT nanocable and (b) SnO_2/MWCNT nanocable at an open circuit potential of 1.5 V in eighth cycle. After Chen et al. [148].

ball-milling [152]. The electrochemical tests on Li/(Si/MWCNT) cells indicate that the highest *C*rev and the lowest *C*irr were obtained 1770 and 469 mA Hg^{-1}, respectively, for the composite anodes made with a ratio of 50% MWCNT: 50% Si. The ball milling contributed to decreasing the sizes of MWCNTs and Si particles, and thus to increasing the electrical contact between these components, which in turn enhanced the Li capacity and cyclic performance. Similarly excellent results have also been reported of the Si/CB/SWCNT nanocomposites that were prepared by dispersing SWCNTs via high power ultrasonication into a pre-milled Si/C composite mixture, followed by a subsequent thermal treatment [153]. The nanocomposite with a nominal composition of 35 wt.% Si/36 wt.% SWCNTs exhibited a remarkable reversible discharge capacity of ~900 mA Hg^{-1} with a negligible capacity loss of 0.3% per cycle up to 30 cycles.

The capacity of pure CNT anode can be increased by filling the CNT interior with high-capacity Li-storage compounds, such as those derived from Sn, Sb, alloys and metal oxides, see e.g. co-axial SnO_2 tube/CNT nanostructure [142] discussed in Section 4.3.4. The nanocomposites of CNT filled with Sn_2Sb alloys showed an impres-

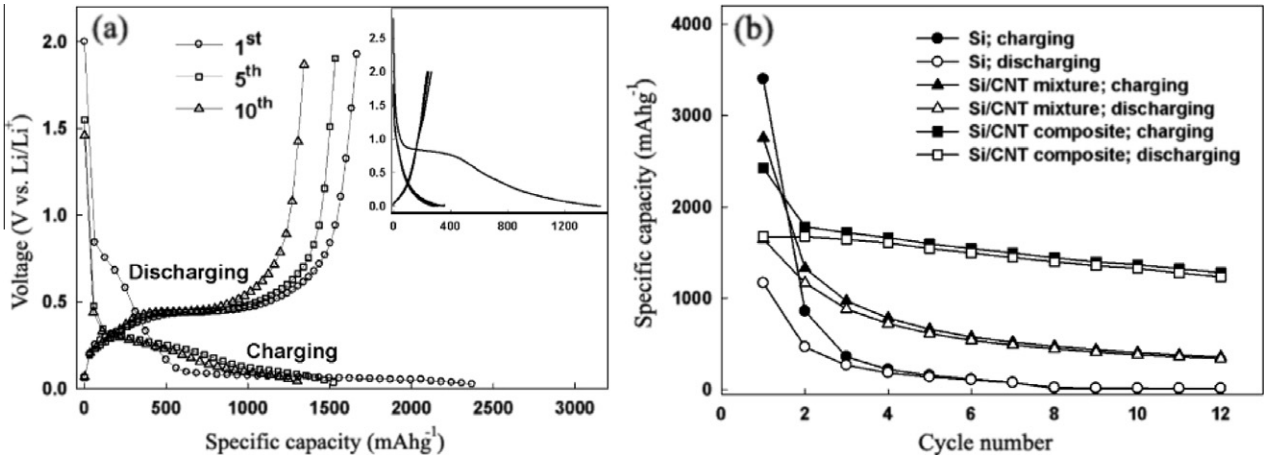

Fig. 30. (a) Galvanostatic charge–discharge voltage curves of Si/MWCNT composite anode (Profiles of pure MWCNT anode are presented in inset). (b) Cycle performance of Si/MWCNT composite anode compared to those of bare Si and Si/MWCNT mixed anodes. After Kim et al. [151].

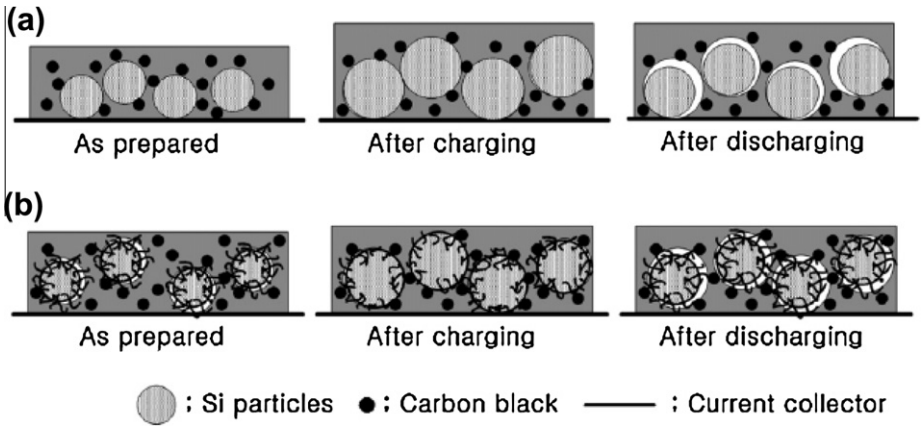

Fig. 31. Schematic illustrations of failure modes encountered in Si anode materials: (a) normal Si and (b) Si/MWCNT nanocomposite. After Kim et al. [151].

sive capacity for Li storage through alloy formation, but were significantly less cycleable than graphite: their first cycle discharge capacity was 1250 mA Hg^{-1} while the corresponding charge capacity was 580 mA Hg^{-1} [154]. It is believed that a carefully crafted combination of CNTs and high-capacity Li-storage compounds may work synergistically to deliver both high capacity and good cycleability. Sn-filled MWCNTs were synthesized using two different methods, including an $NaBH_4$-reduction process and a hydrothermal process, as anode material [117]. At a current rate of 0.1 C, the hydrothermally-filled CNTs gave a first-cycle discharge and charge capacities of 1916 and 834 mA Hg^{-1}, respectively; while the $NaBH_4$-reduced samples gave much higher values of 2474 and 889 mA Hg^{-1}. It is also interesting to note that the charge–discharge capabilities of the Sn-filled CNTs nanocomposites were much higher than the corresponding values, 1281 and 340 mA Hg^{-1}, respectively, of those containing open-ended CNTs. These observations indicate that the electrochemical performance of CNT-metal composites is related to their structural characteristics: metal-filled CNTs are superior to metal-CNT composite mixtures, when used as the anode material for LIBs.

4.4. CNT arrays as anode material

MWCNTs consist of more than two graphene sheets rolled into closed and concentric 1D cylinders. The graphene sheets have an inter-planar spacing of ca. 0.34 nm, which is wide enough for the intercalation/extraction of Li ions. MWCNT arrays have received much attention for use as anode material due to their large surface area and ordered electrode configuration [155]. A few studies have been reported on the fabrication and evaluation of "free-standing" CNT paper electrodes without substrate. The free-standing CNT paper electrodes are light, flexible, highly conductive, and can be fabricated using a simple filtration method under a positive pressure without having to use a metal substrate or binder [156,157]. An added advantage is that the electrode made from buckypaper is much lighter than conventional electrodes that are normally fabricated by coating a mixture containing an active material onto a metal substrate.

There have been increasing interests in flexible and safe energy storage devices based on both batteries and supercapacitors to meet stringent requirements driven mainly by high-power and high-energy applications. One of the potential solutions to these demands is combining the storage capabilities of LIBs together with the excellent power discharge characteristics of capacitors, making the device highly capable of storing useful quantities of electricity that can be discharged very quickly. Once the integrated structure of the electrochemical devices containing three essential components, namely electrodes, spacer and electrolyte, is made mechanically flexible, they can be embedded into various functional systems in a wide range of innovative products such as smart cards, displays and implantable medical devices. A paper-thin and flexible energy storage device was successfully fabricated [158] by incorporating nanoporous cellulose as the main constituent of paper with CNTs. The novelty of this device lies in its mechanical flexibility allowing to change its shape to meet the space requirements of modern devices, as well as the elegance of

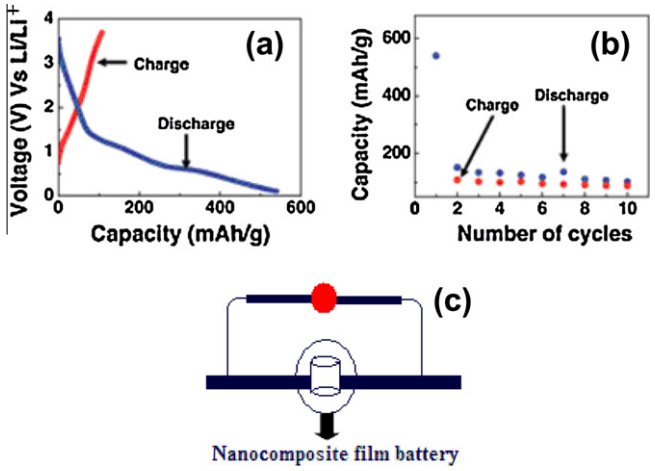

Fig. 32. Electrochemical properties of nanocomposite thin-film paper battery: (a) first charge–discharge curves of the samples cycled between 3.6 and 0.1 V at 10 mA g^{-1}; (b) charge capacity vs. number of cycles; and (c) flexible nanocomposite film battery used to glow a red light-emitting diode (LED). After Pushparaj et al. [158].

the design, where all components, i.e. electrodes, electrolyte and separator, are integrated into a single unit that acts as a building block for the final battery structure. CNT films of uniform thicknesses were grown vertically on a silicon substrate, which were then impregnated with cellulose to form a nanocomposite paper. The paper was assembled into a battery by (i) evaporating a thin layer of Li metal as the anode, (ii) using a Li conducting organic solution as the electrolyte, and (iii) attaching aluminum foil on both sides to collect the current. It was claimed that the supercapacitor could be combined with batteries to make hybrid devices. The charge–discharge cycles of the battery were measured between 3.6 and 0.1 V, at a constant current of 10 mA g^{-1}. A large irreversible-capacity (~430 mA Hg^{-1}) was observed during the first charge–discharge cycle (Fig. 32a), and further charge–discharge cycles resulted in a reversible capacity of 110 mA Hg^{-1} (Fig. 32b). The laminated battery device was able to light up a red light emitting diode (LED) (Fig. 32c) several tens of cycles, demonstrating its excellent discharge performance.

Although they can be used to produce innovative functional nanostructures, aligned CNTs (ACNTs) grown on a substrate suffer from a lack of good electrical connectivity between them [159]. To avoid the lack of lateral connectivity, a novel approach was developed to form a nanostructured ACNT/conducting polymer composite, where the ACNTs were held together by a conducting polymer layer. The ACNTs remained vertically oriented and protruded from the conducting polymer layer with 90% of the tube length being exposed. These free-standing ACNT/poly(3,4-ethylenedioxythiophene (PEDOT)/poly(vinylidene fluoride) (PVDF) membrane electrode was not only lightweight, flexible, highly conductive and mechanically robust, but also could be fabricated into a rechargeable battery without having to use a metal substrate. In addition, the capacity of the ACNT/PEDOT/PVDF electrode was 50% higher than that observed for a free-standing SWCNT paper. This study has important implications in the development of ACNT/conducting polymer composites as a new class of electrode material for flexible rechargeable LIBs and may find niche applications of CNTs in flexible electronic devices.

5. Concluding remarks and future prospect

As LIBs find a diverse range of new applications, such as EVs, HEVs and power tools, they must have excellent rate charge–discharge performance, as well as high energy and power densities. To achieve this ultimate goal, there have been enormous research efforts aimed at improving LIB technology, especially the electrode performance. Nanoscaled materials represent a rapidly growing area in the field of LIBs because of their substantial advantages in terms of mass transport. Transport in nanoparticle systems typically encompasses shorter transport lengths for both electrons and Li ions, larger electrode–electrolyte contact area and better accommodation of the strains arising from Li ion insertion/extraction [3,88,97,160–163]. However, a large surface area may also increase the solvent decomposition occurring at both the anode and cathode during charge–discharge cycles, resulting in a large, irreversible capacity loss. In addition, poor packing of nanoparticles may also lead to a low volumetric energy density. Therefore, it is important that the particle size and morphology be optimized so as to maximize the performance of the electrode material. The addition of CNTs in conventional electrodes, both cathodes and anodes, can enhance the electronic conductivity, improve Li diffusion and maintain morphological stability, which in turn result in higher reversible capacities, rate capability and battery cycleability. However, there are also challenges in the synthesis of CNT-based nanocomposites, which include: (i) poor adhesion of nanoparticles with CNTs; (ii) difficulties in uniform dispersion; and (iii) a low CNT content that can be incorporated without agglomeration. Other important challenges include the development of environment-friendly, low-cost, high-volume synthesis and fabrication techniques for nanocomposites, as well as the significant improvement in safety characteristics for their use in the battery systems. As has been verified for many electrode materials, such as $Li_4Ti_5O_{12}$ and $LiMn_2O_4$ [164–166], an electronic conductive medium, such as Ag, could greatly improve their discharge capacity and cyclic stability at high rates. However, Ag is very expensive and the synthetic route of the composites is difficult to control for homogeneity of the components. While carbon materials are more cost effective than Ag, the graphitizing process influences the yield of the composites. As a key new material, CNT–based nanocomposites have been studied extensively due to their excellent multifunctional characteristics as electrode materials.

Graphene, a one-atom-thick planar sheet of carbon that is densely packed in a honeycomb crystal lattice, has emerged recent years as an alternative to other carbon allotropes, including CNTs, after the development of various routes for synthesis [167–170]. Due to its combination of unique physical, electrical, mechanical and other functional characteristics, graphene will surely contribute to achieving the ultimate performance of future LIBs and other energy storage devices. Indeed, the application of graphene or graphene oxide in electrode materials for LIBs and supercapacitors has already appeared in the literature [171–174]. Because it is highly conductive, mechanically robust, non-toxic, chemically and thermally tolerant, and has a large electrochemical stability window, graphene is particularly suited for Li ion storage to replace the traditional graphite anodes, for serving as template supporting the active anode particles [149,172], and acting as conductive additive in LIBs [173]. The most obvious impediment to commercial exploitation of graphene materials for LIBs is the absence of reliable methods for large-scale production of processable graphene sheets. Commercially viable synthetic strategies must be explored in order to translate laboratory findings into devices.

The rational design of novel electrical energy storage systems with a high energy density will benefit from a combined experimental and theoretical approach. Nanostructuring the electrode materials together with incorporation of conducting fillers like CNTs for larger surface areas and thus higher intercalating capacities is a promising strategy in advanced LIBs. This gives rise to various advantages, including (i) fast rate capabilities due to shorter lengths for both electronic and Li ionic transport, (ii) high energy density and excellent cyclic life arising from the large electrode/

electrolyte contact area, as well as (iii) better accommodation of the swelling strains resulting from the Li ion insertion/extraction processes. However, the high interparticle contact resistance caused by the aggregation between the nanostructured active materials and embedded CNTs limits the efficiency of electronic conduction and thereby reduces the power density. A revolutionary advance is necessary for efficient design of hybrid nanostructured materials that best utilize the characteristics of both materials taking into account their relative advantages and weaknesses. Progress in these key areas will eventually allow developing new materials with high energy and high power at low costs, which will in turn accelerate the innovation in battery systems.

Acknowledgements

This work was supported by the Research Grants Council (Project code: 614010, 613811) and the Innovation and Technology Fund (Project code: GHP/028/08SZ) of Hong Kong SAR, as well as Finetex-HKUST R & D Center (Project code: FTG001-MECH.07/08). Technical assistance from the Materials Characterization and Preparation Facilities (MCPF), HKUST is appreciated.

References

[1] Scrosati B. Challenge of portable power. Nature 1995;373:557–8.
[2] Tarascon JM, Armand M. Issues and challenges facing rechargeable batteries. Nature 2001;414:359–67.
[3] Arico AS, Bruce P, Scrosati B, Tarascon JM, Van Schalkwijk W. Nanostructured materials for advanced energy conversion and storage devices. Nat Mater 2005;4:366–77.
[4] Bruce PG, Scrosati B, Tarascon JM. Nanomaterials for rechargeable lithium batteries. Angew Chem Int Ed 2008;47:2930–46.
[5] Kang K, Meng YS, Breger J, Grey CP, Ceder G. Electrodes with high power and high capacity for rechargeable lithium batteries. Science 2006;311:977–80.
[6] Whittingham MS. Lithium batteries and cathode materials. Chem Rev 2004;104:4271–301.
[7] Jiang C, Hosono E, Zhou H. Nanomaterials for lithium ion batteries. Nano Today 2006;1:28–33.
[8] Whittingham MS. Materials challenges facing electrical energy storage. MRS Bull 2008;33:411–9.
[9] Wallace GG, Chen J, Mozer AJ, Forsyth M, MacFarlane DR, Wang C. Nanoelectrodes: energy conversion and storage. Mater Today 2009;12:20–7.
[10] Li H, Wang Z, Chen L, Huang X. Research on advanced materials for Li-ion batteries. Adv Mater 2009;21:4593–607.
[11] Frackowiak E, Gautier S, Gaucher H, Bonnamy S, Beguin F. Electrochemical storage of lithium multiwalled carbon nanotubes. Carbon 1999;37:61–9.
[12] Chen J, Minett AI, Liu Y, Lynam C, Sherrell P, Wang C, et al. Direct growth of flexible carbon nanotube electrodes. Adv Mater 2008;20(3):566–70.
[13] Claye A, Fischer J, Huffman C, Rinzler A, Smalley RE. Solid-state electrochemistry of the Li single wall carbon nanotube system. J Electrochem Soc 2000;147:2845–52.
[14] Liu P, Hornyak GL, Dillon AC, Gennett T, Heben MJ, Turner JA. Electrochemical performance of carbon nanotube materials in lithium ion batteries. J Electrochem Soc: Proc Int Symp 1999:31–9.
[15] Hsoeh HM, Tai NH, Lee CY, Chen JM, Wang FT. Electrochemical properties of the multi-walled carbon nanotube electrode for secondary lithium-ion battery. Rev Adv Mater Sci 2003;5:67–71.
[16] Iijima S. Helical microtubules of graphitic carbon. Nature 1991;354:56–8.
[17] Lin Y, Taylor S, Li H, Shiral Fernando KA, Qu L, Wang W. Advances toward bioapplications of carbon nanotubes. J Mater Chem 2004;14:527–41.
[18] Moniruzzaman M, Winey KI. Polymer nanocomposites containing carbon nanotubes. Macromolecules 2006;39:5194–205.
[19] Bethune DS, Johnson RD, Salem RJ, de Varies MS, Yannoni CS. Amtoms in carbon cages: the structure and properties of endohedral fullerenes. Nature 1993;366:123–8.
[20] Journet C, Maser WK, Bernier P, Loiseau A, de la Chapelle ML, Lefrant S. Large-scale production of single-walled carbon nanotubes by the electric-arc technique. Nature 1997;388:756–8.
[21] Rinzler AG, Liu J, Dai H, Nikolaev P, Huffman CB, Rodriguez-Macias FJ. Large-scale purification of single-wall carbon nanotubes: process, product and characterization. Appl Phys A 1998;67:29–37.
[22] Nikolaev P, Bronikowski MJ, Bradley RK, Fohmund F, Colbert DT, Smith KA. Gas-phase catalytic growth of single-walled carbon nanotubes from carbon monoxide. Chem Phys Lett 1999;313:91–7.
[23] Ren ZF, Huang ZP, Xu JW, Wang JH, Bush P, Siegal MP. Synthesis of large arrays of well-aligned carbon nanotubes on glass. Science 1998;282:1105–7.
[24] Thostenson ET, Ren ZF, Chou TW. Advances in the science and technology of CNTs and their composites: a review. Compos Sci Technol 2001;61:1899–912.
[25] Qian D, Wagner GJ, Liu WK, Yu MF, Ruoff RS. Mechanics of carbon nanotubes. Appl Mech Rev 2002;55:495–533.
[26] Ajayan PM, Schadler LS, Braun PV. Nanocomposite science and technology. Weinheim (Germany): Wiley-VCH, Verlag GmbH & Co.; 2003.
[27] Nalwa HS. Handbook of nanostructured materials and nanotechnology, vol. 5. New York (USA): Academic Press; 2000.
[28] Ma PC, Kim JK. Carbon nanotubes for polymer reinforcement. Singapore: CRC Press and Taylor & Francis; 2011.
[29] Ma PC, Kim JK, Tang BZ. Conversion of semiconducting behavior of carbon nanotubes using ball milling. Chem Phys Lett 2008;458:166–9.
[30] Ma PC, Wang SQ, Tang BZ, Kim JK. In-situ amino functionalization of carbon nanotubes using ball milling. J Nanosci Nanotechnol 2009;9:749–53.
[31] Pistoia G, Zane D, Zhang Y. Some aspects of $LiMn_2O_4$ electrochemistry in the 4 V range. J Electrochem Soc 1995;142:2551–7.
[32] Resimers JN, Dahn JR, von Sacken U. Effects of impurities on the electrochemical properties of $LiCoO_2$. J Electrochem Soc 1993;140:2752–4.
[33] Li W, Resimers JN, Dahn JR. In situ X-ray diffraction and electrochemical studies of $Li_{1-x}NiO_2$. Solid State Ionics 1993;67:123–30.
[34] Dahn JR, von Sacken U, Juzkow MW, Al-Janaby H. Rechargeable $LiNiO_2$/carbon cells. J Electrochem Soc 1991;138:2207–11.
[35] Koetschau I, Richard MN, Dahn JR, Soupart JB, Rousche JC. Orthorhombic $LiMnO_2$ as a high capacity cathode for Li-ion cells. J Electrochem Soc 1995;142:2906–10.
[36] Jeong IS, Kim JU, Gu HB. Electrochemical properties of $LiMg_yMn_{2-y}O_4$ spinel phases for rechargeable lithium batteries. J Power Sources 2001;102:55–9.
[37] Jin B, Kim JU, Gu HB. Electrochemical properties of lithium–sulfur batteries. J Power Sources 2003;117:148–52.
[38] Kim JU, Jo YJ, Park GC, Gu HB. Charge/discharge characteristics of $LiMnO_2$ composite for lithium polymer battery. J Power Sources 2003;119–121:686–9.
[39] Suresh P, Shukla AK, Munichandraiah N. Characterization of Zn- and Fe-substituted $LiMnO_2$ as cathode materials in Li-ion cells. J Power Sources 2006;161:1307–13.
[40] Suresh P, Shukla AK, Munichandraiah N. Electrochemical properties of $LiMn_{1-x}M_xO_2$ (M = Ni, Al, Mg) as cathode materials in lithium-ion cells. J Electrochem Soc 2005;152:A2273–80.
[41] Rodrigues S, Munichandraiah N, Shukla AK. Novel solution–combustion synthesis of $LiCoO_2$ and its characterization as cathode material for lithium-ion cells. J Power Sources 2001;102:322–5.
[42] Suresh P, Rodrigues S, Shukla AK, Sivashankar SA, Munichandraiah N. Synthesis of $LiCo_{1-x}Ni_xO_2$ from a low temperature solution combustion route and characterization. J Power Sources 2002;112:665–70.
[43] Padhi AK, Nanjundaswamy KS, Goodenough JB. Phospho-olivines as positive-electrode materials for rechargeable lithium batteries. J Electrochem Soc 1997;144:1188–94.
[44] Bramnik NN, Bramnik KG, Buhrmester T, Baehtz C, Ehrenberg H, Fuess H. Electrochemical and structural study of $LiCoPO_4$-based electrodes. J Solid State Electrochem 2004;8:558–64.
[45] Jin B, Gu HB, Kim KW. Effect of different conductive additives on charge/discharge properties of $LiCoPO_4$/Li batteries. J Solid State Electrochem 2008;12:105–11.
[46] Shiraishi K, Dokko K, Kanamura K. Formation of impurities on phospho-olivine $LiFePO_4$ during hydrothermal synthesis. J Power Sources 2005;146:555–8.
[47] Myung ST, Komaba S, Hirosaki N, Yashiro H, Kumagai N. Emulsion drying synthesis of olivine $LiFePO_4$/C composite and its electrochemical properties as lithium intercalation material. Electrochim Acta 2004;49:4213–22.
[48] Yim SC, Edwards R, Taylor N, Herle PS, Nazar LF. Dimensional reduction: synthesis and structure of layered $Li_5M(PO_4)_2F_2$ (M = V, Cr). Chem Mater 2006;18:1745–52.
[49] Ellis BL, Makahnouk WRM, Makimura Y, Toghill K, Nazar LF. A multifunctional 3.5 V iron-based phosphate cathode for rechargeable batteries. Nat Mater 2007;6:749–53.
[50] Barker J, Gover RKB, Burns P, Bryan AJ. Hybrid ion. A lithium-ion cell based on a sodium insertion material. Electrochem Solid-State Lett 2006;9:A190–2.
[51] Recham N, Chotard JN, Dupont L, Delacourt C, Walker W, Armand M, et al. A 3.6 V lithium-based fluorosulphate insertion positive electrode for lithium-ion batteries. Nat Mater 2010;9:68–74.
[52] Wang G, Zhang Q, Yu Z, Qu M. The effect of different kinds of nano-carbon conductive additives in lithium ion batteries on the resistance and electrochemical behavior of the $LiCoO_2$ composite cathodes. Solid State Ionics 2008;179:263–8.
[53] Li X, Kang F, Shen W. A comparative investigation on multiwalled carbon nanotubes and carbon black as conducting additive in $LiNi_{0.7}Co_{0.3}O_2$. Electrochem Solid-State Lett 2006;9:A126–9.
[54] Li X, Kang F, Shen W. Multiwalled carbon nanotubes as a conducting additive in a $LiNi_{0.7}Co_{0.3}O_2$ cathode for rechargeable lithium batteries. Carbon 2006;44:1334–6.
[55] Sheem K, Lee YH, Lim HS. High-density positive electrodes containing carbon nanotubes for use in Li-ion cells. J Power Sources 2006;158:1425–30.
[56] Huang ZD, Liu XM, Zhang B, Oh SW, Wong SK, Kim JK. $LiNi_{1/3}Co_{1/3}Mn_{1/3}O_2$ with novel 1D nanoporous structure: high power cathode material for rechargeable Li ion batteries. Scripta Mater 2011;64:122–5.
[57] Huang ZD, Liu XM, Oh SW, Zhang B, Ma PC, Kim JK. Microscopically porous, interconnected single crystal $LiNi_{1/3}Co_{1/3}Mn_{1/3}O_2$ cathode material for lithium ion batteries. J Mater Chem 2011;21:10777–84.

[58] Varzi A, Täubert C, Wohlfahrt-Mehrens M, Kreis M, Schütz W. Study of multi-walled carbon nanotubes for lithium-ion battery electrodes. J Power Sources 2011;196:3303–9.

[59] Jin B, Gu HB, Zhang W, Park KH, Sun G. Effect of different carbon conductive additives on electrochemical properties of $LiFePO_4$–C/Li batteries. J Solid State Electrochem 2008;12:1549–54.

[60] Li X, Kang F, Bai X, Shen W. A novel network composite cathode of $LiFePO_4$/multiwalled carbon nanotubes with high rate capability for lithium ion batteries. Electrochem Commun 2007;9:663–6.

[61] Wang L, Huang Y, Jiang R, Jia D. Nano-$LiFePO_4$/MWCNT cathode materials prepared by room-temperature solid-state reaction and microwave heating. J Electrochem Soc 2007;154:A1015–1019.

[62] Kim SW, Ryu J, Park CB, Kang K. Carbon nanotube-amorphous $FePO_4$ core–shell nanowires as cathode material for Li ion batteries. Chem Commun 2010:7409–11.

[63] Liu S, Zhang J, Huang K, Yu J. Improvement of electrochemical performance of $LiMn_2O_4$ composite cathode by ox-MWCNT addition for Li-ion battery. J Braz Chem Soc 2008;19:1078–83.

[64] Liu XM, Huang ZD, Oh S, Ma PC, Chan PCH, Kumar G, et al. Sol–gel synthesis of multiwalled carbon nanotube-$LiMn_2O_4$ nanocomposites as cathode materials of Li-ion batteries. J Power Sources 2010;195:4290–6.

[65] Sivakkumar SR, MacFarlane DR, Forsyth M, Kim DW. Ionic liquid-based rechargeable lithium metal–polymer cells assembled with polyaniline/carbon nanotube composite cathode. J Electrochem Soc 2007;154:A834–8.

[66] Cochet M, Maser WK, Benito AM, Callejas MA, Martinez MT, Benoit JM, et al. Synthesis of a new polyaniline/nanotube composite: "*in-situ*" polymerisation and charge transfer through site–selective interaction. Chem Commun 2001;16:1450–1.

[67] Wang CY, Mottaghitalab V, Too CO, Spinks GM, Wallace GG. Polyaniline and polyaniline–carbon nanotube composite fibres as battery materials in ionic liquid electrolyte. J Power Sources 2007;163:1105–9.

[68] He BL, Dong B, Wang W, Li HL. Performance of polyaniline/multi-walled carbon nanotubes composites as cathode for rechargeable lithium batteries. Mater Chem Phys 2009;114:371–5.

[69] Cheng F, Tang W, Li C, Chen J, Liu H, Shen P, et al. Conducting poly(aniline) nanotubes and nanofibers: controlled synthesis and application in lithium/poly(aniline) rechargeable batteries. Chem Eur J 2006;12:3082–8.

[70] Shan Y, Gao L. Multiwalled carbon nanotubes/Co_3O_4 nanocomposites and its electrochemical performance in lithium storage. Chem Lett 2004;33:1560–1.

[71] Baibarac M, Lira-Cantú M, Oró Sol J, Baltog I, Casañ-Pastor N, Gomez-Romero P. Poly(N-vinyl carbazole) and carbon nanotubes based composites and their application to rechargeable lithium batteries. Compos Sci Technol 2007;67:2556–63.

[72] Han SC, Song MS, Lee H, Kim HS, Ahn HJ, Lee JY. Effect of multiwalled carbon nanotubes on electrochemical properties of lithium/sulfur rechargeable batteries. J Electrochem Soc 2003;150:A889–93.

[73] Besenhard JO, Yang J, Winter M. Will advanced lithium-alloy anodes have a chance in lithium-ion batteries? J Power Sources 1997;68:87–90.

[74] Winter M, Besenhard JO. Electrochemical lithiation of tin and tin-based intermetallics and composites. Electrochim Acta 1999;45:31–50.

[75] Winter M, Besenhard JO, Spahr ME, Novak P. Insertion electrode materials for rechargeable lithium batteries. Adv Mater 1998;10:725–63.

[76] Obrovac MN, Christensen L. Structural changes in silicon anodes during lithium insertion/extraction. Electrochem Solid State Lett 2004;7:A93–6.

[77] Hatchard TD, Dahn JR. In-situ XRD and electrochemical study of the reaction of lithium with amorphous silicon. J Electrochem Soc 2004;151:A838–42.

[78] Beaulieu LY, Eberman KW, Turner RL, Krause LJ, Dahn JR. Colossal reversible volume changes in lithium alloys. Electrochem Solid State Lett 2001;4:A137–40.

[79] Yoshio M, Wang H, Fukuda K, Umeno T, Dimov N, Ogumi Z. Carbon-coated Si as a lithium-ion battery anode material. J Electrochem Soc 2002;149:A1598–603.

[80] Kim JW, Ryu JH, Lee KT, Oh SM. Improvement of silicon powder negative electrodes by copper electroless deposition for lithium secondary batteries. J Power Sources 2005;147:227–33.

[81] Dimov NN, Fukuda K, Umeno T, Kugino S, Yoshio M. Characterization of carbon-coated silicon: structural evolution and possible limitations. J Power Sources 2003;114:88–95.

[82] Ryu JH, Kim JW, Sung YE, Oh SM. Failure modes of silicon powder negative electrode in lithium secondary batteries. Electrochem Solid State Lett 2004;7:A306–9.

[83] Liu WR, Yang MH, Wu HC, Chiao SM, Wu NL. Enhanced cycle life of Si anode for Li-ion batteries by using modified elastomeric binder. Electrochem Solid State Lett 2005;8:A100–3.

[84] Liu Y, Matsumura T, Imanishi N, Hirano A, Ichikawa T, Takeda Y. Preparation and characterization of Si/C composite coated with polyaniline as novel anodes for Li-ion batteries. Electrochem Solid State Lett 2005;8:A599–602.

[85] Guo ZP, Milin E, Wang JZ, Chen J, Liu HK. Silicon/disordered carbon nanocomposites for lithium-ion battery anodes. J Electrochem Soc 2005;152:A2211–6.

[86] Wu YP, Rahm E, Holze R. Carbon anode materials for lithium ion battery. J Power Sources 2003;114:228–36.

[87] Morcrette M, Rozier P, Dupont L, Mugnier E, Sannier L, Galy J, et al. A reversible copper extrusion–insertion electrode for rechargeable Li batteries. Nat Mater 2003;2:755–61.

[88] Poizot P, Laruelle S, Grugeon S, Dupont L, Tarascon JM. Nano-sized transition-metal oxides as negative-electrode materials for lithium-ion batteries. Nature 2000;407:496–9.

[89] Mosby JM, Prieto AL. Direct electrodeposition of Cu_2Sb for lithium-ion battery anodes. J Am Chem Soc 2008;130:10656–61.

[90] Zhang WM, Hu JS, Guo YG, Zheng SF, Zhong LS, Song WG, et al. Tin-nanoparticles encapsulated in elastic hollow carbon spheres for high-performance anode material in lithium-ion batteries. Adv Mater 2008;20:1160–5.

[91] Che G, Lakshmi BB, Fisher ER, Martin CR. Carbon nanotubule membranes for electrochemical energy storage and production. Nature 1998;393:346–9.

[92] Wu GT, Wang CS, Zhang XB, Yang HS, Qi ZF, He PM, et al. Structure and lithium insertion properties of carbon nanotubes. J Electrochem Soc 1999;146:1696–701.

[93] Maurin G, Bousquet C, Henn F, Bernier P, Amairac R, Simon B. Electrochemical intercalation of lithium into multiwall carbon nanotubes. Chem Phys Lett 1999;312:14–8.

[94] Ishihara T, Kawahara A, Nishiguchi H, Yoshio M, Takita Y. Effect of synthesis condition of graphitic nanocarbon tube on anodic property of Li-ion rechargeable battery. J Power Sources 2001;97–98:129–32.

[95] Frackowiak E, Gautier S, Gaucher H, Bonnamy S, Beguin F. Electrochemical storage of lithium in multiwalled carbon nanotubes. Carbon 1999;37:61–9.

[96] Yang ZH, Wu HQ. Electrochemical intercalation of lithium into carbon nanotubes. Solid State Ionics 2001;143:173–80.

[97] Odani A, Nimberger A, Markovsky B, Sominski E, Levi E, Kumar VG, et al. Development and testing of nanomaterials for rechargeable lithium batteries. J Power Sources 2003;119–121:517–21.

[98] Raffaelle RP, Landi BJ, Harris JD, Bailey SG, Hepp AF. Carbon nanotubes for power applications. Mater Sci Eng B 2005;116:233–43.

[99] Mi CH, Cao GS, Zhao XB. A non-GIC mechanism of lithium storage in chemical etched MWNTs. J Electroanal Chem 2004;562:217–21.

[100] Shimoda H, Gao B, Tang XP, Kleinhammes A, Fleming L, Wu Y, et al. Lithium intercalation into ethched single-wall carbon nanotubes. Physica B 2002;323:133–4.

[101] Eom JY, Kim DY, Kwon HS. Effects of ball-milling on lithium insertion into multi-walled carbon nanotubes synthesized by thermal chemical vapour deposition. J Power Sources 2006;157:507–14.

[102] Gao B, Bower C, Lorentzen JD, Fleming L, Kleinhammes A, Tang XP, et al. Enhance saturation lithium composition in ball-milled single-walled carbon nanotubes. Chem Phys Lett 2000;327:69–75.

[103] Wang XX, Wang JN, Chang H, Zhang YF. Preparation of short carbon nanotubes and application as an electrode material in Li-ion batteries. Adv Funct Mater 2007;17:3613–8.

[104] Wang XX, Wang JN, Su LF. Preparation and electrochemical performance of ultra-short carbon nanotubes. J Power Sources 2009;186:194–200.

[105] Yang S, Huo J, Song H, Chen X. A comparative study of electrochemical properties of two kinds of carbon nanotubes as anode materials for lithium ion batteries. Electrochim Acta 2008;53:2238–44.

[106] Kaskhedikar NA, Maier J. Lithium storage in carbon nanostructures. Adv Mater 2009;21:2664–80.

[107] Lv R, Zou L, Gui X, Kang F, Zhu Y, Zhu H, et al. High-yield bamboo-shaped carbon nanotubes from cresol for electrochemical application. Chem Commun 2008:2046–8.

[108] Zhou J, Song H, Fu B, Wu B, Chen X. Synthesis and high-rate capability of quadrangular carbon nanotubes with one open end as anode materials for lithium-ion batteries. J Mater Chem 2010;20:2794–800.

[109] Mukhopadhyay I, Hoshino N, Kawasaki S, Okino F, Hsu WK, Touhara H. Electrochemical Li insertion in B-doped multiwall carbon nanotubes. J Electrochem Soc 2002;149:A39–44.

[110] Landi BJ, DiLeo RA, Schauerman CM, Cress CD, Ganter MJ, Raffaelle RP. Multi-walled carbon nanotube paper anodes for lithium ion batteries. J Nanosci Nanotechnol 2009;9:3406–10.

[111] Carrol DL, Redlich P, Blase X, Charlier JC, Curran S, Ajayan PM, et al. Effects of nanodomain formation on the electronic structure of doped carbon nanotubes. Phys Rev Lett 1998;81:2332–5.

[112] Wei B, Spolenak R, Kohler-Redlich P, Ruhle M, Artz E. Electrical transport in pure and boron-doped carbon nanotubes. Appl Phys Lett 1999;74:3149–52.

[113] Mui SC, Trapa PE, Huang B, Soo PP, Lozow MI, Wang TC, et al. Block copolymer-templated nanocomposite electrodes for rechargeable lithium batteries. J Electrochem Soc 2002;149:A1610–5.

[114] Lee SW, Yabuuchi N, Gallant BM, Chen S, Kim BS, Hammond PT, et al. High-power lithium batteries from functionalized carbon-nanotube electrodes. Nat Nanotechnol 2010;5:531–7.

[115] Gnanaraj S, Pol VG, Gedanken A, Aurbach D. Improving the high-temperature performance of $LiMn_2O_4$ spinel electrodes by coating the active mass with MgO via a sonochemical method. Electrochem Commun 2003;5:940–5.

[116] Aurbach D, Markovsky B, Rodkin A, Cojocaru M, Levi E, Kim HJ. An analysis of rechargeable lithium-ion batteries after prolonged cycling. Electrochim Acta 2002;47:1899–911.

[117] Kumar TP, Ramesh R, Lin YY, Fey GTK. Tin-filled carbon nanotubes as insertion anode materials for lithium-ion batteries. Electrochem Commun 2004;6:520–5.

[118] Guo ZP, Zhao ZW, Liu HK, Dou SX. Electrochemical lithiation and de-lithiation of MWNT–Sn/SnNi nanocomposites. Carbon 2005;43:1392–9.

[119] NuLi Y, Yang J, Jiang M. Synthesis and characterization of Sb/CNT and Bi/CNT composites as anode materials for lithium-ion batteries. Mater Lett 2008;62:2092–5.
[120] Chen WX, Lee JY, Liu ZL. The nanocomposites of carbon nanotube with Sb and $SnSb_{0.5}$ as Li-ion battery anodes. Carbon 2003;41:959–66.
[121] Park MS, Needham SA, Wang GX, Kang YM. Park, JS, Dou SX, Liu HK. Nanostructured SnSb/carbon nanotube composites synthesized by reductive precipitation for lithium-ion batteries. Chem Mater 2007;19:2406–10.
[122] Xie J, Zhao XB, Cao GS, Zhao MJ. Electrochemical performance of $CoSb_3$/MWNTs nanocomposite prepared by in situ solvothermal synthesis. Electrochim Acta 2004;50:2725–31.
[123] Zhai C, Du N, Zhang H, Yu J, Wu P, Xiao C, et al. Assembling $CoSn_3$ nanoparticles on multiwalled carbon nanotubes with enhanced lithium storage properties. Nanoscale 2011;3:1798–801.
[124] Yin JT, Wada M, Kitano Y, Tanase S, Kajita O, Sakai T. Nanostructured Ag–Fe–Sn/carbon nanotubes composites as anode materials for advanced lithium-ion batteries. J Electrochem Soc 2005;152:A1341–6.
[125] Huang H, Zhang WK, Gan XP, Wang C, Zhang L. Electrochemical investigation of TiO_2/carbon nanotubes nanocomposite as anode materials for lithium-ion batteries. Mater Lett 2007;61:296–9.
[126] Yan J, Song H, Yang S, Yan J, Chen X. Preparation and electrochemical properties of composites of carbon nanotubes loaded with Ag and TiO_2 nanoparticle for use as anode material in lithium-ion batteries. Electrochim Acta 2008;53:6351–5.
[127] An G, Na N, Zhang X, Miao Z, Miao S, Ding K, et al. SnO_2/carbon nanotube nanocomposites synthesized in supercritical fluids: highly efficient materials for use as a chemical sensor and as the anode of a lithium-ion battery. Nanotechnology 2007;18:435707-1–435707-12.
[128] Fu Y, Ma R, Shu Y, Cao Z, Ma X. Preparation and characterization of SnO_2/carbon nanotube composite for lithium ion battery applications. Mater Lett 2009;63:1946–8.
[129] Huang J, Jiang Z. The preparation and characterization of $Li_4Ti_5O_{12}$/carbon nanotubes for lithium ion battery. Electrochim Acta 2008;53:7756–9.
[130] Poizot P, Laruelli S, Grugeon S, Dupont L, Tarascon JM. Nano-sized transition-metal oxides as negative electrode materials for lithium-ion batteries. Nature 2000;407:496–9.
[131] Tarascon JM, Grugeon S, Morcrette M, Laruelle S, Rozier P, Poizot P. New concepts for the search of better electrode materials for rechargeable lithium batteries. CR Chem 2005;8:9–15.
[132] Taberna PL, Mitra S, Poizot P, Simon P, Tarascon JM. High rate capabilities Fe_3O_4-based Cu nano-architectured electrodes for lithium-ion battery applications. Nat Mater 2006;5:567–73.
[133] Li J, Tang S, Lu L, Zeng HC. Preparation of nanocomposites of metals, metal oxides and carbon nanotubes via self-assembly. J Am Chem Soc 2007;129:9401–9.
[134] Wang G, Shen X, Yao J. One-dimensional nanostructures as electrode materials for lithium-ion batteries with improved electrochemical performance. J Power Sources 2009;189:543–6.
[135] He Y, Huang L, Cai JS, Zheng XM, Sun SG. Structure and electrochemical performance of nanostructured Fe_3O_4/carbon nanotube composites as anodes for lithium ion batteries. Electrochim Acta 2010;55:1140–4.
[136] Marschilok A, Lee CY, Subramanian A, Takeuchi KJ, Takeuchi ES. Carbon nanotube substrate electrodes for lightweight, long-life rechargeable batteries. Energy Environ Sci 2011;4:2943–51.
[137] Landi BJ, Ganter MJ, Cress CD, Dileo RA, Raffaelle RP. Carbon nanotubes for lithium ion batteries. Energy Environ Sci 2009;2:638–54.
[138] Armstrong AR, Armstrong G, Canales J, Bruce PG. TiO_2-B nanowires. Angew Chem Int Ed 2004;43:2286–8.
[139] Kim YA, Kojima M, Muramatsu H, Umemoto S, Watanabe T, Yoshida K, et al. In-situ Raman study on single- and double-walled carbon nanotubes as a function of lithium insertion. Small 2006;2:667–76.
[140] Li JR, Tang ZL, Zhang ZT. Layered hydrogen titanate nanowires with novel lithium intercalation properties. Chem Mater 2005;17:5848–55.
[141] Hu YS, Kienle L, Guo YG, Maier J. High lithium electroactivity of nanometer-sized rutile TiO_2. Adv Mater 2006;18:1421–6.
[142] Sudant G, Baudrin E, Larcher D, Tarascon JM. Electrochemical lithium reactivity with nanotextured anatase-type TiO_2. J Mater Chem 2005;15:1263–9.
[143] Lee DH, Kim DW, Park JG. Enhanced rate capabilities of nanobrookite with electronically conducting MWCNT networks. Cryst Growth Des 2008;8:4506–10.
[144] Cao FF, Guo YG, Zheng SF, Wu XL, Jiang LY, Bi RR, et al. Symbiotic coaxial nanocables: facile synthesis and an efficient and elegant morphological solution to the lithium storage problem. Chem Mater 2010;22:1908–14.
[145] Zhang WJ. A review of the electrochemical performance of alloy anodes for lithium-ion batteries. J Power Sources 2010;196:13–24.
[146] Wang Y, Zeng HC, Lee JY. Highly reversible lithium storage in porous SnO_2 nanotubes with coaxially grown carbon nanotube overlayers. Adv Mater 2006;18:645–9.
[147] Wen Z, Wang Q, Zhang Q, Li J. In situ growth of mesoporous SnO_2 on multiwalled carbon nanotubes: a novel composite with porous-tube structure as anode for lithium batteries. Adv Funct Mater 2007;17:2772–8.
[148] Chen G, Wang Z, Xia D. One-pot synthesis of carbon nanotube@SnO_2-Au coaxial nanocable for lithium-ion batteries with high rate capability. Chem Mater 2008;20:6951–6.
[149] Zhang B, Zheng QB, Huang ZD, Oh SW, Kim JK. SnO2-graphene-carbon nanotube mixture for anode material with improved rate capacities. Carbon 2011;49:4524–34.
[150] Li H, Huang XJ, Chen LQ, Wu ZG, Liang Y. A high capacity nano-Si composite anode material for lithium rechargeable batteries. Electrochem Solid-State Lett 1999;2:547–9.
[151] Kim T, Mo YH, Nahm KS, Oh SM. Carbon nanotubes (CNTs) as a buffer layer in silicon/CNTs composite electrodes for lithium secondary batteries. J Power Sources 2006;162:1275–81.
[152] Eom JY, Park JW, Kwon HS, Rajendran S. Electrochemical insertion of lithium into multiwalled carbon nanotube/silicon composites produced by ballmilling. J Electrochem Soc 2006;153:A1678–84.
[153] Wang W, Kumta PN. Reversible high capacity nanocomposite anodes of Si/C/SWNTs for rechargeable Li-ion batteries. J Power Sources 2007;172:650–8.
[154] Chen WX, Lee JY, Liu Z. Electrochemical lithiation and de-lithiation of carbon nanotube-Sn_2Sb nanocomposites. Electrochem Commun 2002;4:260–5.
[155] Zhao J, Gao QY, Gu C, Yang Y. Preparation of multi-walled carbon nanotube array electrodes and its electrochemical intercalation behavior of Li ions. Chem Phys Lett 2002;358:77–82.
[156] Morris RS, Dixon BG, Gennett T, Raffaelle R, Heben MJ. High-energy, rechargeable Li-ion battery based on carbon nanotube technology. J Power Sources 2004;138:277–80.
[157] Ng H, Wang J, Guo ZP, Chen J, Wang GX, Liu HK. Single wall carbon nanotube paper as anode for lithium-ion battery. Electrochim Acta 2005;51:23–8.
[158] Pushparaj VL, Shaijumon MM, Kumar A, Murugesan S, Ci L, Vajtai R, et al. Flexible energy storage devices based on nanocomposite paper. Proc Nation Acad Sci USA 2007;104:13574–7.
[159] Chen J, Liu Y, Minett A, Lynam C, Wang J, Wallace GG. Flexible, aligned carbon nanotube/conducting polymer electrodes for a lithium-ion battery. Chem Mater 2007;19:3595–7.
[160] Maier J. Nanoionics: ion transport and electrochemical storage in confined systems. Nat Mater 2005;4:805–15.
[161] Zhukovskii YF, Balaya P, Kotomin EA, Maier J. Evidence for interfacial-storage anomaly in nanocomposites for lithium batteries from first-principles simulations. Phys Rev Lett 2006;96:0583021–24.
[162] Maier J. Mass storage in space charge regions of nano-sized systems. Faraday Discuss 2007;134:51–66.
[163] Zhao N, Fu L, Yang L, Zhang T, Wang Gn, Wu Y, et al. Nanostructured anode materials for Li-ion batteries. Pure Appl Chem 2008;80:2283–95.
[164] Huang SH, Wen ZY, Zhu XJ, Gu ZH. Preparation and electrochemical performance of Ag doped $Li_4Ti_5O_{12}$. Electrochem Commun 2004;6:1093–7.
[165] Son JT, Park KS, Chung HT, Kim HG. Surface-modification of $LiMn_2O_4$ with a silver–metal coating. J Power Sources 2004;126:182–5.
[166] Huang S, Wen Z, Yang X, Zhu X, Lin B. Synthesis and the improved high-rate performance of $LiMn_2O_4$/Ag composite cathode for lithium-ion batteries. Electrochem Solid-State Lett 2006;9:A443–447.
[167] Stankovich S, Dikin DA, Dommett GHB, Kohlhaas KM, Zimney EJ, Stach EA, et al. Graphene-based composite materials. Nature 2006;442:282–6.
[168] Geim AK, Novoselov KS. The rise of graphene. Nat Mater 2007;6:183–91.
[169] Geng Y, Wang SJ, Kim JK. Preparation of graphite nanoplatelets and graphene sheets. J Colloid Interface Sci 2009;336:592–8.
[170] Zheng QB, Ip WH, Lin XY, Yousefi N, Yeung KK, Kim JK, et al. Transparent conductive films consisting of ultralarge graphene sheets produced by Langmuir–Blodgett assembly. ACS Nano 2011;5:6039–51.
[171] Lian PC, Zhu XF, Liang SZ, Li Z, Yang WS, Wang HH. Large reversible capacity of high quality graphene sheets as an anode material for lithium-ion batteries. Electrochim Acta 2010;55:3909–14.
[172] Wu ZS, Ren WC, Wen L, Gao LB, Zhao JP, Chen ZP. Graphene anchored with Co_3O_4 nanoparticles as anode of lithium ion batteries with enhanced reversible capacity and cyclic performance. ACS Nano 2010;4:3187–94.
[173] Su FY, You CH, He YB, Lv W, Cui W, Jin FM, et al. Flexible and planar graphene conductive additives for lithium-ion batteries. J Mater Chem 2010;20:9644–50.
[174] Liang MH, Zhi LJ. Graphene-based electrode materials for rechargeable lithium batteries. J Mater Chem 2009;19:5871–8.